Published in final edited form as:
Dev Biol. 2007 April 1; 304(1): 156–181. doi:10.1016/j.ydbio.2006.12.029.

A molecular analysis of neurogenic placode and cranial sensory ganglion development in the shark, *Scyliorhinus canicula*

P. O'Neill[1], **R. B. McCole**, and **C. V. H. Baker**[*]
Department of Physiology, Development and Neuroscience, Anatomy Building, Downing Street, Cambridge CB2 3DY, United Kingdom

Abstract

In order to gain insight into the evolution of the genetic control of the development of cranial neurogenic placodes and cranial sensory ganglia in vertebrates, we cloned and analysed the spatiotemporal expression pattern of six transcription factor genes in a chondrichthyan, the shark *Scyliorhinus canicula* (lesser-spotted dogfish/catshark). As in other vertebrates, *NeuroD* is expressed in all cranial sensory ganglia. We show that *Pax3* is expressed in the profundal placode and ganglion, strongly supporting homology between the separate profundal ganglion of elasmobranchs and basal actinopterygians and the ophthalmic trigeminal placode-derived neurons of the fused amniote trigeminal ganglion. We show that *Pax2* is a conserved pan-gnathostome marker for epibranchial and otic placodes, and confirm that *Phox2b* is a conserved pan-gnathostome marker for epibranchial placode-derived neurons. We identify *Eya4* as a novel marker for the lateral line system throughout its development, expressed in lateral line placodes, sensory ridges and migrating primordia, neuromasts and electroreceptors. We also identify *Tbx3* as a specific marker for lateral line ganglia in shark embryos. We use the spatiotemporal expression pattern of these genes to characterise the development of neurogenic placodes and cranial sensory ganglia in the dogfish, with a focus on the epibranchial and lateral line placodes. Our findings demonstrate the evolutionary conservation across all gnathostomes of at least some of the transcription factor networks underlying neurogenic placode development.

Introduction

Vertebrates (craniates) are unique within the chordates in possessing a well-defined head, containing a relatively large brain protected by a cartilaginous or bony braincase, as well as complex paired sense organs: olfactory organs, eyes, inner ears, and the mechanoreceptive and electroreceptive lateral line system (lost in amniotes). As previously emphasised (Northcutt and Gans, 1983; Gans and Northcutt, 1983; also see Northcutt, 2005), these and several other defining vertebrate characteristics are, for the most part, derived during embryogenesis from neural crest cells and cranial placodes. Cranial placodes are discrete patches of thickened ectoderm in the embryonic head; they give rise to all paired peripheral sense organs (olfactory organ, inner ear, lateral line system) and the neurons that provide

[*]Address for manuscript correspondence: Clare V. H. Baker, Ph.D., Physiology, Development & Neuroscience, Anatomy Building, Downing Street, Cambridge, CB2 3DY, U.K. Tel ++44 (0)1223 333789, Fax ++44 (0)1223 333786. cvhb1@cam.ac.uk.
[1]Current address: Laboratory for Sensory Development, Center for Developmental Biology (CDB), RIKEN Kobe Institute, 2-2-3 Minatojima-minamimachi, Chuo-ku, Kobe, Hyogo 650-0047, Japan

Europe PMC Funders Author Manuscripts

their afferent innervation, plus the lenses of the paired eyes and the endocrine adenohypophysis (reviewed in Baker and Bronner-Fraser, 2001; Schlosser, 2006). Cranial placodes also form somatosensory neurons in the profundal and trigeminal ganglia, and visceral sensory neurons in the geniculate, petrosal and nodose ganglia. Visceral sensory neurons provide afferent innervation for taste buds (which are not placode-derived) as well as the afferent arm of visceral reflex circuits (reviewed in Baker and Bronner-Fraser, 2001; Brunet and Pattyn, 2002; Schlosser, 2006). Hence, vertebrate cranial placode-derived neurons and sense organs are crucial for relaying both external and internal stimuli to the central nervous system. The evolution of cranial placodes, and neural crest cells, was important for the radical innovations in sensory and skeletal organization that accompanied the transition of vertebrate ancestors from small, benthic ciliary filter-feeders to large, active predators (Northcutt and Gans, 1983; Gans and Northcutt, 1983; Northcutt, 2005).

Despite the crucial importance of cranial placodes for the formation of the vertebrate sensory nervous system, placode development was relatively neglected for many decades after their discovery in the early 1880s in shark embryos (van Wijhe, 1882). More recently, the availability of molecular markers for different stages of placode development has enabled rapid advances in our understanding of the cellular and molecular mechanisms underlying adenohypophyseal, olfactory, lens, and otic placode development in model organisms such as mouse, chick, *Xenopus* and zebrafish (reviewed in Baker and Bronner-Fraser, 2001; Schlosser, 2006). The trigeminal placodes (which form somatosensory neurons) and epibranchial placodes (which form visceral sensory neurons in the geniculate, petrosal and nodose ganglia) have also received some attention, particularly in chick and, more recently, zebrafish (reviewed in Baker and Bronner-Fraser, 2001; Schlosser, 2006). The formation of the mechanosensory lateral line system is also being studied intensively in zebrafish, although the main focus is on the control of posterior lateral line primordium migration along the embryo trunk (arguably the most spectacular example of migration in vertebrate embryonic development; e.g. David et al., 2002; Haas and Gilmour, 2006). In general, though, much remains to be learned at all stages of placode development.

Different placodes are induced by different tissues and molecules at different times during development, and give rise to very different derivatives (see Graham and Begbie, 2000; Baker and Bronner-Fraser, 2001; Streit, 2004; Schlosser, 2006). Nonetheless, they all share a common developmental origin, from a horseshoe-shaped strip of ectoderm around the edge of the anterior neural plate, known variously as the pre-placodal region or pan-placodal domain (reviewed in Baker and Bronner-Fraser, 2001; Streit, 2004; Bailey and Streit, 2006; Schlosser, 2006). This strip of ectoderm is defined molecularly at the early neurula stage by the overlapping expression of the transcription factor/co-factor genes *Six1/2*, *Six4/5* and *Eya1/2*; it may represent a region of placodal bias, and/or of competence to respond to individual placode-inducing signals (for detailed discussions, see Bailey and Streit, 2006; Schlosser, 2006; also see Martin and Groves, 2006).

Six and *Eya* genes are part of a complex regulatory network with *Dach* and *Pax* genes that was first described in the context of *Drosophila* eye development (reviewed in Rebay et al., 2005). Six proteins are homeodomain transcription factors that interact with the transcription co-factors Eya and Dach; Eya proteins are also protein tyrosine phosphatases whose activity

converts Dach from a co-repressor to a co-activator of Six (reviewed in Rebay et al., 2005). *Six*, *Eya* and *Dach* gene family members are all co-expressed in the vertebrate preplacodal region and maintained in individual placodes, while different *Pax* genes (encoding paired domain transcription factors) are upregulated later in cells fated to adopt different placodal fates, e.g. *Pax6* in prospective lens and olfactory placode cells (though it is downregulated in olfactory placode cells; Bhattacharyya et al., 2004), *Pax3* in ophthalmic trigeminal placode cells, *Pax8* and *Pax2* in future otic and epibranchial placode cells (reviewed in Baker and Bronner-Fraser, 2001; Streit, 2004; Bailey and Streit, 2006; Schlosser, 2006). This raises the possibility that specific *Pax* genes are important for individual placode identity. Indeed, the maintenance of *Pax6*, *Pax3* and *Pax2* expression in prospective lens, ophthalmic trigeminal, and otic placode cells, respectively, does seem to correlate with adoption of specific placode identity (Baker and Bronner-Fraser, 2000; Baker et al., 2002; Bhattacharyya et al., 2004; Ohyama et al., 2006). However, the precise roles in placode development of these and other molecular markers are not well understood; for example, relatively few downstream targets are known. Also, the mechanisms by which the preplacodal region is subdivided into individual placodes (cell movement, cell sorting, etc) remain to be elucidated.

Another topic of great interest, and continuing debate, is how vertebrate placodes evolved, and whether or not homologues of vertebrate placodes can be found in the invertebrate chordates, such as ascidians and amphioxus (see Baker and Bronner-Fraser, 1997; Baker and Schlosser, 2005; Schlosser, 2005). As emphasised previously (Baker and Bronner-Fraser, 1997; Baker and Schlosser, 2005), patches of thickened neurogenic ectoderm (i.e., neurogenic placodes) are found across the animal kingdom. Hence, finding placodes in invertebrate chordates is not, in itself, informative about the evolution of vertebrate cranial placodes. Instead, the important questions (to our minds) are, firstly, in non-vertebrate chordates and deuterostomes, what is the origin of the cell types (or evolutionary precursors of such cell types) that in vertebrates are derived from cranial placodes, and secondly, how did these come to develop in vertebrates from discrete patches of cranial ectoderm? In answering such questions, and trying to assign homologies, it is essential to have a good understanding of the genetic mechanisms underlying the formation of the preplacodal domain, different placodes, and different placode-derived cell types. It is also important to know to what extent these mechanisms are conserved across the vertebrates as a whole. Most of our understanding of the molecular control of cranial placode development comes from tetrapods (mouse, chick, and *Xenopus*), though the ever-increasing number of studies on placode development in zebrafish (a recent euteleost) supports the idea of a pan-vertebrate conservation of genetic mechanisms (e.g. Hans et al., 2004; Mackereth et al., 2005). Nonetheless, very little is known about the expression of known early placode marker genes in more basal vertebrates, apart from one study showing that lamprey *Pax2* is expressed in the otic placode, and that a lamprey *Pax3/7* gene is expressed in the trigeminal placode (McCauley and Bronner-Fraser, 2002).

Here, we provide the first molecular analysis of placode development in chondrichthyan embryos, using the shark *Scyliorhinus canicula* as a model. Not only do sharks belong to one of the most basal extant vertebrate groups, it seems only appropriate to bring molecular tools to bear on placode development in the vertebrate group in which they were first discovered, almost 125 years ago (van Wijhe, 1882). The development of shark placodes and their

associated ganglia has been described in detail, based on morphology alone (e.g. Landacre, 1916; Johnson, 1917), while the development of shark cranial nerves has also been described more recently based on neurofilament antibody staining (Kuratani and Horigome, 2000). In this paper, we complement and extend these studies with a molecular analysis of the development of neurogenic placodes and placode-derived sensory ganglia in the lesser-spotted dogfish (catshark), *Scyliorhinus canicula*.

Materials and Methods

Collection and staging of embryos

Scyliorhinus canicula eggs were obtained from the Marine Biological Association, Plymouth, UK or from the University of Glasgow Marine Biological Station Millport, Isle of Cumbrae, UK and kept at 15°C in oxygenated seawater. Embryos were dissected and staged according to Ballard et al. (1993), prior to fixation in 4% paraformaldehyde (PFA) overnight at 4°C. Specimens were dehydrated and stored in methanol at -20°C.

Production of cDNA

RNA from a pool of 5 dogfish embryos between stages 22-27 (Ballard et al., 1993) was used to make cDNA under RNAase-free conditions. A 15μl mix containing 4μl RNA, 0.5μg random primers (Promega) was incubated at 70°C for 5 minutes, then made to final 25μl final volume with 1X M-MLV RT buffer (Roche), 1mM dNTPs (Bioline), 25U M-MLV reverse transcriptase (Roche). The reverse transcription reaction was performed at 37°C for 1 hour; completed reaction mix was diluted 1:10 with RNase-free water (Sigma).

Primer design, PCR and sequencing

Degenerate primers were designed either manually from sequence alignments (MacVector) or using CODEHOP (Rose et al., 2003; http://blocks.fhcrc.org/codehop.html). Primer sequences are given in Table 1. The primers were used in PCR reactions on *S. canicula* cDNA using Sigma Jump Start™ RedTaq DNA Polymerase. The cycling programme was 94°C for 5 minutes, 40 cycles of 94°C for 30 seconds, annealing temperature (specific to each primer) for 40 seconds, 72°C for 1 minute, and finally 72°C for 10 minutes. Touchdown PCR was performed for combinations of primers in order to produce more specific products: 94°C for 2 minutes, then 5 'touchdown' cycles of 94°C for 30 seconds, annealing temperature starting at 61°C and reduced by 1°C each cycle for 40 seconds, 72°C for 1 minute, then 35 normal cycles of 94°C for 30 seconds, 55°C for 1 minute, 72°C for 1 minute, then a final 72°C for 10 minutes. The amplified fragments were purified either using the Qiagen Qiaquick PCR purification kit or by performing larger-scale reactions, running the entire product on a 1% agarose gel, excising the band using a sterile scalpel and purifying the DNA using the Qiagen Minelute Gel Extraction Kit. 25ng purified DNA fragments were ligated into pGEM®-T Easy Vector (Promega) according to the manufacturer's instructions. The ligations were then used to transform Subcloning Efficiency™ DH5α™ (Invitrogen) or JM109 (Promega) chemically competent *E. coli*. Plasmids were purified using the Promega Wizard Plus SV Miniprep Kit and sequenced by the Department of Biochemistry, University of Cambridge. Sequence results were analysed using BLAST (http://www.ncbi.nlm.nih.gov/BLAST/) and MacVector.

Wholemount *in situ* hybridisation

Antisense RNA probes were transcribed using T7 or SP6 RNA polymerases (Roche) in conjunction with digoxigenin- or fluorescein-conjugated dUTPs (Roche) following standard protocols. Dogfish embryos were rehydrated through a methanol gradient into diethylpyrocarbonate (DEPC)-treated phosphate-buffered saline (PBS) (100%, 75%, 50%, 25% methanol in DEPC-PBS), then treated with 20μg of proteinase K for 25 minutes at room temperature. Following washing in DEPC-PBS, embryos were re-fixed in 4% PFA/DEPC-PBS for 15 minutes at room temperature, and washed in PBS, then in 2xSSC (0.3M NaCl, 0.03M sodium citrate). Specimens were prehybridised in hybridisation solution (1x salt solution [0.2M NaCl, 10mM Tris pH7.5, 5mM $NaH_2PO_4.H_20$, 5mM Na_2HPO_4, 5mM EDTA], 50% formamide, 10% dextran sulphate, 1mg/ml yeast tRNA, 1x Denhardt's Solution) for 1 hour at room temperature. Hybridisation was performed overnight at 70°C with a 1:2500 dilution of the transcription reaction. Embryos were washed 4 times for 30 minutes each at 70°C in wash solution (50% formamide, 1xSSC, 0.1% Tween-20), then twice for 20 minutes at room temperature in MABT (0.1M maleic acid, 150mM NaCl, 0.1% Tween-20, pH 7.5). After blocking for 2 hours at room temperature in 20% sheep serum (Sigma), 2% Boehringer blocking reagent in MABT, embryos were incubated overnight at 4°C with a 1:2000 dilution (0.0375U) of anti-digoxigenin or anti-fluorescein antibody (Roche) in blocking buffer, then washed in MABT (two quick rinses then five 30-minute washes) and equilibrated in NTMT (100mM NaCl, 100mM Tris pH 9.5, 50mM $MgCl_2$, 0.1% Tween-20). The colour reaction was initiated by adding 100μl NBT/BCIP (Roche) in 5ml NTMT to the embryos, and stopped by transferring to PBS. Embryos were rinsed once in PBS, post-fixed in 4% PFA for 10 minutes and returned to PBS for photographing.

Sectioning wholemount *in situ* embryos

Embryos were transferred from PBS to 5% sucrose in PBS, 15% sucrose and finally 15% sucrose, 7.5% gelatin in PBS and kept at 44°C before being poured into moulds and positioned for transverse sectioning through the head and allowed to cool. 20μm sections were produced using a cryostat and mounted on Superfrost Plus slides (VWR) using Fluoromount G (SouthernBiotech).

In situ hybridisation on slides

Embryos were immersed in 100% methanol (30 minutes, 3 times), then Histosol (National Diagnostics; 30 minutes, 3 times) then paraffin wax (Raymond Lamb, UK; 1 hour, 3 times at 60°C), before being transferred to plastic moulds and positioned for transverse sectioning. 10μm sections on Superfrost Plus slides (VWR) were produced using a rotary microtome. Slides were dewaxed in Histosol (5 minutes, twice), then rehydrated through a methanol gradient as above. Slides were digested with 5μg/ml proteinase K for 5 minutes, then washed with DEPC-PBS, fixed in 4% PFA for 10 minutes then washed again in PBS. Prehybridisation and hybridisation were performed as described for whole-mount *in situ* hybridisation, under coverslips in a slide incubator (Boekel) humidified with 50% formamide, 2X SSC. Slides were rinsed three times for 30 minutes each in wash solution at 70°C, then twice at room temperature in MABT. Antibody incubation and colour development were performed as described for whole-mount *in situ* hybridisation. Slides

were mounted using Fluoromount G (SouthernBiotech) and photographed using a Zeiss Axioplan 2 microscope and Princetown Instruments Inc. RTE/CCD-1401 camera.

Immunohistochemistry in whole-mount

The protocol used was modified from that of Freitas and Cohn (2004). After three 1-hour washes at room temperature in PBS with 1% Triton-X100 (PBT-1), embryos were incubated in 0.025% trypsin for 2–5 minutes, then immersed for 15 minutes on ice in acetone that had been pre-cooled to -20°C. After rinsing twice for 5 minutes each in ice-cold PBT-1, the specimens were blocked overnight in 10% goat serum, 1% dimethyl sulfoxide and 5% H_2O_2 in PBT-1, then incubated at 4°C for 3 days in 3A10 antibody at 1:500 in PBT-1 with 10% goat serum. (The 3A10 antibody, which recognises a neurofilament-associated antigen, was developed by Tom Jessell and Jane Dodd, obtained from the Developmental Studies Hybridoma Bank developed under the auspices of the NICHD and maintained by the University of Iowa, Department of Biological Sciences, Iowa City, IA 52242.) After three 1-hour washes in PBT-1, the embryos were incubated overnight at 4°C with biotinylated goat anti-mouse IgG (Jackson) at 1:500 in PBT-1 with 1% goat serum. After three 1-hour washes in PBT-1, the embryos were incubated overnight with ABC-complex (Dako, UK). Embryos were washed as before in PBT-1, followed by PBS, before being pre-incubated in 0.5mg/ml diaminobenzidine (DAB; Sigma Fast™ 3,3' diaminobenzidine tablet sets). The colour reaction was developed by transferring embryos to fresh DAB activated with 0.003% H_2O_2, and stopped by transfer into PBS.

Immunohistochemistry on slides

All incubations were at room temperature in a chamber humidified with distilled water. To block, 10% sheep serum (Sigma) in PBS was added to slides for 30 minutes. Slides were incubated for 1 hour in 3A10 antibody (see previous section), diluted 1:1000 in blocking solution. After three 5-minute washes in PBS, slides were incubated for 1 hour with biotinylated goat anti-mouse IgG (Jackson) diluted 1:500 in blocking solution. After three 5-minute washes in PBS, slides were incubated for 30 minutes with ABC-complex (Dako, UK), then washed in PBS as before, and the colour reaction performed in 0.5mg/ml DAB (Sigma Fast™ 3,3' diaminobenzidine tablet sets) activated with 0.003% H_2O_2. The colour reaction was stopped by transfer to PBS; slides were then fixed in 4% PFA for 10 minutes, transferred back to PBS and mounted using Fluoromount G (SouthernBiotech).

DASPEI labelling of neuromasts

Sensory neuromasts of the lateral line system were visualised by immersing living specimens of *S. canicula* (following removal of embryo from egg case) in 1mM DASPEI (Molecular Probes) for 1 hour at 16°C in seawater. Following staining, embryos were transferred to fresh seawater and photographed under epifluorescence.

Results

Isolation of molecular markers of neurogenic placodes and neurons in the shark, *Scyliorhinus canicula*

Using degenerate PCR (primer sequences given in Table 1), we isolated fragments of six transcription factor genes predicted to be expressed in neurogenic placodes and/or cranial sensory ganglia in the shark *Scyliorhinus canicula* (lesser-spotted dogfish/catshark). We cloned *NeuroD* as a putative pan-neuronal marker, *Pax3* as a putative trigeminal placode marker, *Pax2* as a putative otic and epibranchial placode marker, and *Phox2b* as a putative epibranchial placode-derived neuron marker. We isolated *Eya4* in an attempt to clone *Eya1* as a putative pan-placodal marker, and we cloned *Tbx3* as a putative lateral line placode marker. The resultant PCR products were sequenced and their identity determined by BLAST (NCBI) searches and protein alignments (MacVector; Table 2 and Supplementary Figs. 1-6). GenBank accession numbers are given in Table 2. Phylogenetic trees were constructed using the neighbor-joining method (MacVector), with related transcription factors as outgroups, to confirm the identity of cloned gene fragments in each case (Fig. 1).

Position of cranial sensory ganglia in *S. canicula* at stage 28

In order to make sense of the development of neurogenic placodes and cranial sensory ganglia in *S. canicula* using molecular markers, we needed to be confident of the relative positions of the various cranial ganglia and their associated nerves in a late-stage embryo. To this end, we performed whole-mount immunostaining for the neurofilament-associated antigen recognised by the 3A10 antibody, at stage 28 (46-51 days of development; Ballard et al. 1993; Fig. 2). The positions of the cranial ganglia and early nerves in this embryo accord very well with those described in detail for *Squalus acanthias* (spiny dogfish) embryos (Landacre, 1916; Johnson, 1917) and with those described for *Scyliorhinus torazame* by Kuratani and Horigome (2000). Our aim here is to give a general overview; for a comprehensive treatment, the reader is referred to Landacre (1916), and also to Norris and Hughes (1920) for a superb description of *Squalus* cranial nerves and ganglia at the pup stage.

The various cranial sensory ganglia can be divided into different functional classes: the profundal and trigeminal ganglia contain somatosensory neurons; the vestibuloacoustic and lateral line ganglia contain neurons that provide afferent innervation for the mechanosensory and electroreceptive receptor cells of the inner ear and lateral line system; while the epibranchial placode-derived ganglia (geniculate, petrosal and nodose) contain visceral sensory neurons that provide afferent innervation to taste buds and to the heart, lungs and other visceral organs (reviewed in Baker and Bronner-Fraser, 2001; Schlosser, 2006). Neural crest-derived somatosensory neurons are also found in the proximal (root) ganglia of the facial, glossopharyngeal and vagal nerves.

The profundal ganglion is found just posterior to the mid-dorsal border of the eye, while the trigeminal ganglion lies just posterior to the dorsal half of the eye; they are partially obscured in lateral view by the anterodorsal lateral line ganglion (following the nomenclature of Northcutt, 1997; see below; Fig. 2A-C). It has been suggested (see

Schlosser and Northcutt, 2000; Schlosser and Ahrens, 2004; Schlosser, 2006) that the separate profundal and trigeminal ganglia found in many gnathostomes are, respectively, homologous to the ophthalmic and maxillomandibular divisions of the fused amniote trigeminal ganglion. The neurons of these different divisions in amniotes derive from separate ophthalmic trigeminal (opV) and maxillomandibular trigeminal (mmV) placodes, and also from neural crest cells (reviewed in Baker and Bronner-Fraser, 2001; Schlosser, 2006). As we demonstrate later, the expression of *S. canicula Pax3* specifically in the profundal placode and ganglion provides strong support for the proposed homology between the profundal placode and the amniote opV placode.

As mentioned, the profundal and trigeminal ganglia of *S. canicula* lie somewhat medial to the anterodorsal lateral line ganglion. This is a prominent ganglion lying dorsal to the eye (Fig. 2A-C). A description of peripheral lateral line nerve projections from the lateral line ganglia is useful here, for comparison later with the distribution of lateral line neuromasts as revealed by *Eya4* expression (see later, Figs. 7 and 8). The superficial ophthalmic ramus of the anterodorsal lateral line nerve extends rostrally from the ganglion in an arc around the eye, ending near the olfactory capsule; "twigs" can be seen projecting from it to innervate lateral line organs of the supraorbital line (Fig. 2B,C). The buccal ramus of the anterodorsal lateral line nerve extends ventrally from the ganglion to innervate lateral line organs of the infraorbital line (Fig. 2B,C). The otic lateral line ganglion, described by Norris and Hughes (1920) as a conspicuous mass of cells protruding from the posterior edge of the buccal portion of the anterodorsal lateral line ganglion, is not obvious here (though see Figs. 3 and 7). This ganglion supplies the short otic lateral line, which passes lateral to the inner ear, and the spiracular organ, a pouch containing mechanosensory hair cells associated with the spiracle, i.e., first pharyngeal cleft; Norris and Hughes, 1920; Northcutt, 1997).

The caudal edge of the anterodorsal lateral line ganglion is in contact with the rostral edge of the vestibuloacoustic (VIII) ganglion, whose neurons derive from the otic placode and which lies immediately rostral to the otic vesicle; it is partially obscured in lateral view by the otic vesicle. The vestibuloacoustic ganglion in turn is in contact ventrally with the anteroventral lateral line ganglion and the geniculate (VII) ganglion to form the acoustico-facial ganglionic complex (Fig. 2A-C). The geniculate ganglion contains visceral sensory neurons derived from the first epibranchial (geniculate) placode; it lies just behind the first pharyngeal (spiracular) cleft (Fig. 2A-D). The anteroventral lateral line ganglion contains neurons derived from the anteroventral lateral line placode; it lies immediately dorsal to the geniculate ganglion, partially obscuring it from lateral view (Fig. 2B,C). Axons from both the geniculate and anteroventral lateral line ganglia run together as the truncus hyomandibularis (Fig. 2A-D).

The middle lateral line ganglion (derived from the middle lateral line placode; see later) lies beneath the caudal end of the otic vesicle, proximal to the larger visceral sensory petrosal ganglion, which is derived from the second epibranchial, or petrosal, placode (Fig. 2A,B,D). The petrosal ganglion extends to the dorsal border of the second pharyngeal cleft.

The vagus (X) "ganglion" has a thin proximal portion that extends caudally from the glossopharyngeal (IX) root (Fig. 2A,B,D). According to Landacre (1916), it contains root

fibres and the primordium of the neural crest-derived somatosensory jugular (proximal X) ganglion. More distally, five "branchial" ganglia (X_1-X_5) can be seen (Fig. 2A,D). Again according to Landacre (1916), the proximal portions of the first three of these contain lateral line neurons (lateralis ganglia X_1-X_3). Following the nomenclature of Northcutt (1997), the supratemporal lateral line ganglion probably corresponds to Landacre's lateralis ganglion X_1, while the posterior lateral line ganglion probably corresponds to Landacre's lateralis ganglia X_2 and X_3 (not readily apparent as separate ganglia in our specimen). Distally, the five branchial ganglia contain visceral sensory neurons derived from the caudal epibranchial (nodose) placodes located above the remaining pharyngeal clefts (visceral/nodose ganglia X_1-X_5). The first three nodose ganglia are clearly separate (Fig. 2A,D) but the last two are fused proximally (Fig. 2A).

NeuroD expression reveals the development of all placode-derived cranial sensory ganglia

NeuroD is a basic helix-loop-helix proneural transcription factor expressed in all primary neurons and neurogenic placodes in *Xenopus* and other vertebrates (reviewed in Chae et al., 2004). *NeuroD* expression was not detected in *S. canicula* embryos at either stage 15 (12-16 days; 5-6 somites) or 17 (16-20 days; 17-25 somites; data not shown). At stage 19 (22-24 days; 40 somites; Fig. 3A), a salt-and-pepper patch of robust *NeuroD* expression is visible by the otic vesicle, dorsal to the second pharyngeal arch; this probably represents neuroblasts of the otic placode-derived vestibuloacoustic (VIII) ganglion and of the anterodorsal lateral line ganglion. Two fainter, salt-and-pepper patches of expression are also visible more rostrally, one behind the eye and one dorsal to the mandibular arch: these probably represent a few early-forming neuroblasts within the profundal and trigeminal placodes (Fig. 3A).

At stage 21 (26-27 days; Fig. 3B), distinct and widely separated primordia for the profundal and trigeminal ganglia can be seen, the smaller profundal ganglion forming immediately posterior to the mid-dorsal border of the eye, and the larger trigeminal ganglion forming dorsal to the mandibular arch. A dense patch of *NeuroD* expression ventral to the rostral half of the open otic vesicle is prominent; this may include not only the forming vestibuloacoustic ganglion, but also anterodorsal lateral line placode-derived neurons. A patch of staining dorsal to the third arch, beneath the caudal edge of the otic vesicle, is also seen; this is likely to represent neuroblasts from the middle lateral line placode that will go on to form the middle lateral line ganglion (see Fig. 2). A faint patch of *NeuroD* expression can be seen dorsal to the fourth arch, likely to represent neurogenesis in the supratemporal lateral line placode, while scattered *NeuroD*$^+$ cells are visible above the fifth arch; this probably represents the start of neurogenesis in the posterior lateral line placode.

At stage 22 (27-28 days; Fig. 3C), a small, faint patch of *NeuroD* expression can be seen at the dorsorostral edge of the olfactory pit. The separate profundal and trigeminal ganglia are clearly visible behind the eye and dorsal to the mandibular arch, respectively. The trigeminal ganglion is much larger than the profundal ganglion. The prominent patch of *NeuroD* expression at the rostral edge of the otic vesicle probably contains neurons both of the forming vestibuloacoustic and anterodorsal lateral line ganglia. Neurogenesis in the three post-otic lateral line placodes/ganglia is much more distinct: in the middle lateral line

placode/ganglion dorsal to the third arch, in the supratemporal lateral line placode/ganglion dorsal to the fourth pharyngeal arch, and in the posterior lateral line placode/ganglion extending above the fifth and sixth pharyngeal arches. Immediately ventral to the stronger *NeuroD* expression in the post-otic lateral line placodes/ganglia, fainter, more salt-and-pepper expression can be seen dorsocaudal to each pharyngeal pouch (only the second pharyngeal cleft has broken through at this stage). This represents the beginning of neurogenesis in the epibranchial placodes.

At stages 23 (28-30 days; Fig. 3D) and 24 (30-31.5 days; Fig. 3E), *NeuroD* expression in the olfactory pits can still be seen. The profundal and trigeminal ganglia are larger and still widely separated. The anterior portion of the large ganglion rostral to the otic vesicle is probably the anterodorsal lateral line ganglion, becoming more clearly visible in its own right. The geniculate ganglion, derived from the geniculate (first epibranchial) placode, is beginning to form; it is visible as a fainter wedge, caudal to the dorsal edge of the first pharyngeal cleft, and tapering into the first pharyngeal arch. Similar patterns of neurogenesis are seen in the petrosal (second epibranchial) placode dorsocaudal to the second pharyngeal cleft, and in the nodose placodes dorsocaudal to the third, fourth, fifth and sixth pharyngeal pouches (the clefts have not formed yet). Immediately dorsal to the forming epibranchial placode-derived ganglia, such that the borders between them seem indistinct, the three post-otic lateral line ganglia (middle, supratemporal and posterior) can still be seen. The posterior lateral line ganglion is large, extending in a long oval above the fifth and sixth arches.

At stage 25 (31-38 days; around 80 somites; Fig. 3F), and stage 26 (37-42 days; Fig. 3G), the overall picture is much the same, except that the profundal and trigeminal ganglia seem to be closer together. At stage 25 (Fig. 3F), neurogenesis within the epibranchial placodes extends down to around one-third of the length of each arch, although neurogenesis in the most caudal nodose placode (dorsocaudal to the sixth pharyngeal pouch) is more prominent still. At stage 26 (Fig. 3G), *NeuroD* expression in the epibranchial placodes seems to be retracting up each arch, lagging behind in the more caudal arches. Also at stage 26 (Fig. 3G), a spur protrudes from the dorsorostral edge of the ganglionic complex in front of the otic vesicle; this is part of the anterodorsal lateral line ganglion. A faint patch of *NeuroD* expression dorsal to the geniculate ganglion is likely to represent the forming anteroventral lateral line ganglion.

At stage 27 (42-46 days; two different embryos shown in Fig. 3H,I), the ganglia as revealed by *NeuroD* expression may now be compared with the neurofilament expression at stage 28 (46-51 days) shown in Fig. 2. The profundal and trigeminal ganglia, still visible in wholemount view by *NeuroD* expression in the younger stage 27 embryo (Fig. 3H), seem to be obscured in lateral view by the rostral projection of the anterodorsal lateral line ganglion in the older stage 27 embryo(Fig. 3I; also see Fig. 2). The position of the otic lateral line ganglion is tentatively identified, after Norris and Hughes (1920), at the caudoventral edge of the buccal (ventral) portion of the anterodorsal lateral line ganglion (Fig. 3H). The geniculate ganglion and the more faintly stained anteroventral lateral line ganglion above it (see Fig. 2) are in contact with the vestibuloacoustic ganglion, forming the ventral spur of the acousticofacial ganglionic complex, pointing ventrally into the second arch. The vestibuloacoustic ganglion seems no longer to abut the rostral edge of the otic vesicle

(compare Fig. 3H with e.g. Fig. 3F,G); alternatively, *NeuroD* expression has been lost from this portion of the vestibuloacoustic ganglion. The petrosal ganglion is visible as a condensed ball beneath the caudal end of the otic vesicle, in contact dorsally with the middle lateral line ganglion (see Fig. 2). The nodose ganglia are similarly seen as distinct aggregates, although the fourth seems to be fused with the fifth, in which neurogenesis still extends quite far ventrally. The supratemporal lateral line ganglion lies dorsally to the first nodose ganglion. The posterior lateral line ganglion extends as a tapering wedge above the second and third nodose ganglia, but it seems to be separate from them, at least at this stage.

Overall, therefore, *NeuroD* expression provides a good overview of the development of the various placode-derived cranial ganglia in *S. canicula*. However, given the close contact between the different ganglia (in particular in the acoustico-facial ganglionic complex), some individual ganglia are sometimes hard to discern. Molecular markers that distinguish between the different ganglia will be invaluable; we show later that *Phox2b* and *Tbx3* represent two such markers, expressed in epibranchial placode-derived and lateral line placode-derived ganglia, respectively.

Pax3 is expressed in the profundal placode and ganglion, supporting homology with the amniote ophthalmic trigeminal placode

Pax3 is a paired-domain, homeodomain transcription factor that is best known for roles in neural crest and muscle development (reviewed in Chi and Epstein, 2002). It is also expressed in the olfactory pits, at least in amniotes (Goulding et al., 1991; Firnberg and Neubüser, 2002; Relaix et al., 2003; Schlosser and Ahrens, 2004). Furthermore, it is an early marker for the ophthalmic trigeminal (opV) placode and opV placode-derived neurons in chick and *Xenopus* (Stark et al., 1997; Schlosser and Ahrens, 2004). As described in the previous section, the profundal and trigeminal ganglia of anamniotes have been proposed to be homologous, respectively, to the ophthalmic (opV) and maxillomandibular (mmV) divisions of the fused amniote trigeminal ganglion (see detailed discussions in Schlosser and Northcutt, 2000; Schlosser and Ahrens, 2004; Schlosser, 2006). Pax3 is also expressed transiently in migrating neural crest cells, and is subsequently upregulated in neural crest cells in the condensing trigeminal and dorsal root ganglia (see Stark et al., 1997; Baker et al., 2002).

We examined the expression of *S. canicula Pax3* at different embryonic stages using whole-mount *in situ* hybridisation (Fig. 4) and found that its expression domains are highly conserved with other gnathostome embryos. It is expressed in the dorsal neural tube, in newly formed somites and in myotomes (Fig. 4A,D,G,J), and at least transiently in migrating cranial neural crest cells (Fig. 4A,B). It is also expressed in a discrete dorsal region of the olfactory pits (Fig. 4E,H,K) and in the profundal placode and ganglion, supporting the proposed homology of the profundal placode with the amniote opV placode. A detailed description of *Pax3* expression in *S. canicula* embryos follows below.

At stage 19 (22-24 days; Fig. 4A,B), *Pax3* is expressed quite prominently in neural crest cell streams migrating into the first and second arch, and also in a patch of ectoderm adjacent to the midbrain and rostral hindbrain. A few *NeuroD*$^{+}$ cells are also seen in this area at the same stage (Fig. 4C). At stages 23-26 (28-42 days; Fig. 4D,E,G,H,J,K), when compared

with *NeuroD* expression at the same stages (Fig. 4F,I,L), *Pax3* is clearly seen to be expressed in the profundal ganglion, and also in the surface ectoderm, as confirmed by analysis of sections of embryos at stages 25-26 (31-42 days; Fig. 4M-O). Hence, *Pax3* is a specific marker for both the profundal placode and profundal placode-derived neuroblasts in *S. canicula*. Possible faint *Pax3* expression is also seen in the trigeminal ganglion in wholemount (e.g. Fig. 4K); this may represent fainter expression of *Pax3* in ganglionic neural crest cells, as seen in the chick (Stark et al., 1997), although this staining was not strong enough to be seen in sections of whole-mount embryos (not shown).

Hence, in shark neurogenic placodes, *Pax3* is a specific marker of the profundal placode and profundal neuroblasts, as well as being expressed in a discrete region of the olfactory pits. This provides strong supporting evidence for the hypothesis that the profundal placode is homologous to the opV placode of amniotes.

Pax2 is a conserved pan-gnathostome marker for both otic and epibranchial placodes

Pax2, a paired domain transcription factor, is well known as an early otic placode marker (though see Ohyama et al., 2006); it is required, together with Pax8, for otic placode development (Hans et al., 2004; Mackereth et al., 2005). However, it is also expressed in the epibranchial placodes in chick, mouse and *Xenopus* (Baker and Bronner-Fraser, 2000; Ohyama and Groves, 2004; Schlosser and Ahrens, 2004). We examined the expression of *S. canicula Pax2* at different embryonic stages using whole-mount *in situ* hybridisation and found that its expression domains are highly conserved with other gnathostome embryos (Fig. 5). It is expressed in both the otic and epibranchial placodes, as well as in other conserved locations such as the midbrain-hindbrain boundary, spinal cord interneurons, the urogenital tract, the optic stalk and the thyroid gland. A detailed description of *Pax2* expression in *S. canicula* embryos follows below.

At stage 17 (16-20 days; 17-25 somites; Fig. 5A,B), *Pax2* is expressed very faintly in the optic vesicles, and very strongly in a stripe in the region of the midbrain-hindbrain border (Fig. 5A). It is also expressed strongly in a broad patch in the hindbrain region, as well as much more faintly more ventrally in the branchial region, where the branchial arches will subsequently form (Fig. 5A). Sections reveal all the stronger staining to be in the forming otic placode, i.e., thickened surface ectoderm by the hindbrain, with the fainter staining extending ventrally into branchial ectoderm (Fig 5B). By stage 19 (22-24 days; 40 somites; Fig. 5C-E), *Pax2* expression in the optic vesicles has resolved into a stripe at the optic fissure; it is still maintained in the midbrain-hindbrain border, and there is a patch of staining at the ventral tip of the first (mandibular) arch with fainter staining at the rostral edge of the arch (Fig. 5C). The otic placodes, which have begun to invaginate, express *Pax2*: sections reveal strong *Pax2* expression restricted to the dorsomedial region of the otic placodes (Fig 5D). Fainter expression is still seen broadly in the surface ectoderm of the branchial region (Fig 5D,E).

At stage 22 (27-28 days; more than 50 somites; Fig. 5F,G), strong *Pax2* expression is seen in the developing urogenital tract (also seen at stage 19; data not shown). *Pax2* is still expressed in the optic fissure and also in a patch in the dorsal optic cup. *Pax2* expression in the first arch is stronger, both at the rostral edge of the arch and at its base. The dorsomedial

expression domain in the otic placode is maintained. In the second (hyoid), third and fourth branchial arches, ectodermal *Pax2* expression is much stronger, and has resolved as broad dorsal stripes behind the first three pharyngeal clefts/pouches (only the first two clefts have formed): these are the resolving epibranchial placodes. Expression remains faint and ventral more caudally, where the endodermal pouches have not yet contacted the surface ectoderm. A comparison with *NeuroD* expression at the same stage (Fig. 5H) shows the beginning of neurogenesis in the dorsal region of each branchial arch, in a much more restricted domain than *Pax2*.

By stage 23 (28-30 days; Fig. 5I), the first arch expression is disappearing apart from in an oval-shaped patch at the base of the arch, which represents the developing thyroid gland at the midline. The stripes of ectodermal *Pax2* expression in the second and more caudal arches have further resolved, such that the strongest expression is seen immediately caudal to each pharyngeal pouch. Expression is restricted to approximately the dorsal third of each arch except for the most caudal patch, behind the fifth pharyngeal pouch, where the expression domain remains broad.

By stage 24 (30-31.5 days; 64-78 somites; Fig. 5J,K), the stripes of *Pax2* expression in the second and more caudal branchial arches are restricted even further dorsally (except for the most caudal stripe); they now clearly represent the maturing epibranchial placodes: the geniculate placode caudal to the dorsal edge of the first pharyngeal cleft, the petrosal placode caudal to the second pharyngeal cleft, and nodose placodes caudal to each subsequent cleft. The third and fourth nodose placodes extend much further ventrally than the first two; *Pax2* expression in the fourth nodose placode is much stronger than in all the other placodes. *Pax2* expression is still seen in the otic vesicle, which now has a thin dorsocaudal *Pax2*$^{+}$ projection (more prominent at later stages): this is the developing endolymphatic duct, which will eventually open to the surface dorsally (see Fig. 5P,Q). Bilateral stripes of *Pax2* expression are also now visible within the hindbrain and spinal cord: these represent interneuron populations (Burrill et al., 1997). Sections show the restriction of *Pax2* expression to the dorsomedial portion of the otic vesicle, and the epibranchial placode ectoderm (Fig. 5K).

At stage 25 (31-38 days; approx. 80 somites; Fig. 5L,M,O), and stage 26 (37-42 days; Fig. 5P,Q,S), the overall picture is much the same, with further refinement of the epibranchial placode expression pattern: only the fourth nodose placode (caudal to the 6th pharyngeal pouch) extends ventrally, while the other epibranchial placodes are all confined to dorsal patches. The *Pax2*$^{+}$ endolymphatic duct is particularly prominent at stage 26 (Fig. 5P,Q), and scattered *Pax2*$^{+}$ cells are now seen diffusely throughout the embryo: we speculate that these are macrophages or other immune system cells. A comparison with *NeuroD* expression at these stages (Fig. 5N,O,R) confirms that *Pax2* expression co-localises with the more ventral ganglia in the branchial arch region, i.e., the epibranchial placode-derived ganglia; no expression is seen in the lateral line placodes that give rise to the more dorsal series of lateral line ganglia.

Sections at stage 26 (Fig. 5S), co-stained with the 3A10 antibody (which recognises a neurofilament-associated antigen), reveal that *Pax2* expression within the epibranchial

placodes is essentially confined to the ectoderm, with only a few delaminating cells maintaining *Pax2* expression. This correlates well with chick *Pax2* expression (Baker and Bronner-Fraser, 2000). Bilateral *Pax2*$^+$ postmitotic interneuron populations can also be seen at the lateral edges of the hindbrain (Fig. 5S).

Overall, therefore, *Pax2* expression in the neurogenic placodes is highly conserved between shark and other gnathostome embryos, both in the otic and epibranchial placodes.

Phox2b is is a conserved pan-gnathostome marker for epibranchial placode-derived neurons

The homeodomain transcription factor Phox2b is expressed by all epibranchial placode-derived neurons (reviewed in Brunet and Pattyn, 2002). We examined the expression of *S. canicula Phox2b* at different embryonic stages using whole-mount *in situ* hybridisation (Fig. 6) and found that its expression in epibranchial placode-derived neurons is conserved across the gnathostomes. A detailed description follows below.

The first hint of *Phox2b* expression in the epibranchial placode region is seen in scattered cells in the dorsal region of the rostral branchial arches at stage 22 (27-28 days; not shown), in a similar pattern to *NeuroD* (see Fig. 3C). By stage 24 (30-31.5 days; Fig. 6A,B), *Phox2b* expression is seen in tapering wedges immediately caudal to the dorsal edge of each pharyngeal cleft/pouch; expression is stronger and more condensed in the first three branchial arches. The dorsal boundary of each patch of *Phox2b* expression is approximately level with the dorsal edge of each pharyngeal pouch. When compared with *NeuroD* expression at the same stage (Fig. 6C), *Phox2b* is clearly seen to co-localise with the more ventral epibranchial placode-derived ganglia at the dorsal edge of each branchial arch; it is not expressed in the more dorsal lateral line placode-derived or vestibuloacoustic ganglia. Sections show that *Phox2b* is expressed not only in neuroblasts that have already delaminated from the epibranchial placodes, but also in some cells within the placodes themselves (Fig. 6D,E). By stage 26 (37-42 days; Fig. 6G,H), *Phox2b* expression in the epibranchial placode-derived ganglia is much stronger and mostly confined to the dorsal edge of each arch. In contrast, *Phox2b* expression in the most caudal nodose ganglion extends much further ventrally than in the other ganglia. This is still the case at stage 28 (46-51 days; not shown), when the other epibranchial placode-derived ganglia are much more condensed. A comparison with *NeuroD* expression in sections at the level of the otic vesicle (Fig. 6F), and *in situ* hybridisation for *Phox2b* directly on sections of stage 27 and stage 28 embryos (Fig. 6J-L) confirms that *Phox2b* is not expressed in the vestibuloacoustic ganglion and lateral line placode-derived ganglia. This is very clear even where lateral line ganglia are in close contact with *Phox2b*$^+$ epibranchial placode-derived ganglia (as shown in Fig. 6J-L for the anteroventral lateral line ganglion and *Phox2b*$^+$ geniculate ganglion).

Phox2b expression is also visible in two prominent patches in the brain, most clearly at stage 26 (Fig. 6G); this represents the motor nuclei of the oculomotor and trochlear nerves (cranial nerves III and IV). We will present a detailed analysis of *Phox2b* expression in the hindbrain in a subsequent manuscript.

Europe PMC Funders Author Manuscripts

Overall, therefore, *Phox2b* expression in the epibranchial placode-derived ganglia is highly conserved between sharks and other gnathostome embryos.

Eya4 is a novel marker for lateral line placodes, migrating lateral line primordia, neuromasts and electroreceptors

We cloned *Eya4* in an attempt to isolate *Eya1*, a putative pan-placodal marker (Schlosser and Ahrens, 2004). We examined the expression of *S. canicula Eya4* at different embryonic stages using whole-mount *in situ* hybridisation (Figs. 7 and 8), and found that it is a novel marker for the lateral line system throughout its entire development, from placodes to sense organs, as well as being expressed in the otic vesicle, the dermomyotome, hypaxial muscle primordia (including in the pectoral and pelvic fins) and branchial arch muscle primordia. A detailed description follows below.

At stage 22 (27-28 days; not shown), *Eya4* is faintly expressed in the hypaxial region of the somites, and in the otic vesicle. By stage 23 (28-30 days; Fig. 7A,D), *Eya4* expression is also seen in the anterodorsal lateral line placode lying rostral to the otic vesicle, including a rostral projection from it, likely to represent the first stages of formation of the supraorbital sensory ridge. *Eya4* is also expressed faintly in the middle and supratemporal lateral line placodes, and more strongly in the posterior lateral line placode lying above the fifth and sixth branchial arches (Fig. 7A,B,D). A comparison with *NeuroD* and *Pax2* expression at stage 23 (Fig. 7B,C) shows that *Eya4* is not expressed in the epibranchial placodes. Sections of a stage 23 embryo on which double *in situ* hybridisation was performed for both *Eya4* and *Pax2* confirm that *Eya4* is expressed in lateral line placode ectoderm, dorsal to the *Pax2*$^{+}$ epibranchial placodes (Fig. 7D).

At stage 24 (30-31.5 days; Fig. 7E-I), the *Eya4*$^{+}$ anterodorsal lateral line placode has bifurcated and elongated to form two short sensory ridges, the supraorbital ridge (obvious in Fig. 7F; shown in section in Fig. 7G) and the infraorbital ridge (more clearly seen at later stages). *Eya4* expression in the middle, supratemporal and posterior lateral line placodes can still be seen (Fig. 7F,H,I); the main trunk line primordium has not yet begun migrating from the posterior lateral line placode in the embryo shown, although in other embryos migration onto the trunk has already begun at stage 24 (not shown). *Eya4* expression is also seen in the branchial arches (Fig. 7E,F,H) and in the hypaxial (ventral) portion of the somites (Fig. 7E; also see Fig. 7Q-S).

By stage 26 (37-42 days; Fig. 7J,L), the anterodorsal lateral line placode is much larger (Fig. 7J,L). The supraorbital and infraorbital sensory ridges arising from it have extended much further above and below the eye respectively; the infraorbital ridge runs along the length of the upper jaw (Fig. 7J,L). A circular patch of *Eya4* expression projecting from the caudoventral border of the *Eya4*$^{+}$ anterodorsal lateral line placode may represent the otic lateral line placode (Fig. 7L), which gives rise to the otic lateral line ganglion. Still further ventrally (but dorsal to the position of the geniculate ganglion; compare with *NeuroD* expression in Fig. 7K,M), another faint patch of *Eya4* expression is likely to represent the anteroventral lateral line placode. The main trunk line primordium is migrating down the flank at this stage (not shown). *Eya4* expression is also seen in stripes in the middle of each branchial arch that are most likely to be branchial arch muscle primordia (Fig. 7J,L).

By stage 27 (42-46 days; Fig. 7N,O,Q,R), the front of the migrating *Eya4*$^{+}$ main trunk line primordium has already reached a point midway between the pectoral and pelvic finbuds (Fig. 7N,Q). The trailing end of the primordium has left in its wake a line of *Eya4*$^{+}$ neuromast primordia (Fig. 7Q; also see Fig. 8). Sections through the trunk show the *Eya4*$^{+}$ main trunk line primordium at the level of the horizontal myoseptum (midway between the dorsal and ventral tips of the somites; Fig. 7R). A thin line of *Eya4* expression is now seen above the branchial arches (Fig. 7O): this most likely represents the start of the dorsal trunk line, which originates from the posterior lateral line placode (Johnson, 1917). Although in some groups the posterior lateral line placode gives rise to dorsal, middle and ventral trunk lines, we did not see an obvious ventral trunk line in *S. canicula*; similarly, a ventral trunk line was not described in *Squalus*; Johnson, 1917; Norris and Hughes, 1920). *Eya4* expression is also clearly seen both in the dorsal dermomyotome and in the hypaxial portion of the somites (Fig. 7N,Q,R), while *Eya4* expression in branchial arch muscle primordia seems to be more condensed, particularly in the mandibular arch (Fig. 7O).

At stage 28 (46-51 days; Fig. 8A,C,E,F), lateral line neuromasts of both head (Fig. 8A) and trunk (Fig. 8E,F) express *Eya4*, as do the developing ampullary organs (electroreceptors) in the ampullary fields on the head (Fig. 8A). In other gnathostomes, ampullary organs develop from the lateral edges of the sensory ridges that form by elongation of the lateral line placodes (e.g. Northcutt et al., 1994; Gibbs and Northcutt, 2004). At this stage, the dorsal supraorbital, and dorsal and ventral infraorbital ampullary fields are apparent as speckled patches of *Eya4* staining above and below the supraorbital and infraorbital lines of *Eya4*$^{+}$ neuromasts (Fig. 8A). A comparison with neurofilament immunostaining at the same stage (Fig. 8B) shows the "twigs" from the superficial ophthalmic and buccal rami of the anterodorsal lateral line nerve that innervate the *Eya4*$^{+}$ neuromasts of the supraorbital and infraorbital lateral lines, respectively. The migrating posterior lateral line primordium has reached almost to the tip of the tail (Fig. 8C). A comparison with neurofilament immunostaining shows the posterior lateral line nerve extending into the migrating primordium (Fig. 8D), and "twigs" from the nerve more rostrally innervating *Eya4*$^{+}$ neuromasts of the posterior lateral line (Fig. 8E-G). *Eya4* expression can also be seen in wholemount in the hypaxial muscles of both pelvic (Fig. 8E) and pectoral (Fig. 8F) fins.

At stage 29 (49-53 days), *Eya4* expression is similarly maintained in neuromasts, e.g. of the supraorbital and infraorbital lines, as shown in Fig. 8H (compare with neuromasts revealed by DASPEI staining at stage 31 in Fig. 8I), and also in the ampullary organ fields, where it is now clear that *Eya4* is expressed in individual ampullary organs (Fig. 8H). Hypaxial muscle in the pectoral fins (the pelvic fins were not examined at this stage) can still be seen in whole-mount to express *Eya4* (Fig. 8J).

At stage 31 (60-80 days), *Eya4* expression can still be seen in neuromasts (Fig. 8K,L) and ampullary organs (Fig. 8K). Sections show that only a few cells in each neuromast express *Eya4* (Fig. 8L,M): based on their central position within the neuromast, these are most likely to be hair cells. *Eya4* is also expressed in the spiracular organ (data not shown), in the sensory epithelium of the inner ear (perhaps also in hair cells), and in the vestibuloacoustic ganglion (Fig. 8M).

Overall, therefore, within the cranial placodes, *Eya4* is a novel marker for the lateral line system at all stages. It is expressed in lateral line placodes and maintained in lateral line placode-derived sense organs, including the mechanosensory hair cells of neuromasts, and electroreceptive ampullary organs. *Eya4* is also expressed in the sensory epithelium of the inner ear and in the vestibuloacoustic ganglion.

Tbx3 is expressed in lateral line and vestibuloacoustic ganglia in *S. canicula*

Tbx3 encodes a T-box transcription factor that is a member of the closely related subgroup of *Tbx2/3* and *Tbx4/5* genes, best known for their involvement in limb development (reviewed in Naiche et al., 2005; King et al., 2006). *Xenopus Tbx3* was reported to be expressed in cranial ganglia and the "lateral line organ" (Li et al., 1997; Takabatake et al., 2000), although Schlosser and Ahrens (2004) disputed this, suggesting that lateral line placodes had been wrongly identified as cranial ganglia, and hypaxial muscle primordium as the posterior lateral line organ. We cloned *Tbx3* as a putative lateral line placode marker. We examined the expression of *S. canicula Tbx3* at different embryonic stages using whole-mount *in situ* hybridisation (Figs. 9 and 10). Its expression pattern is, in general, conserved with other gnathostome embryos, e.g. in the pineal gland, dorsal retina, neurohypophysis, otic vesicle, mesenchyme around the olfactory placodes, pectoral and pelvic fin buds, and posterior notochord (Chapman et al., 1996; Li et al., 1997; Gibson-Brown et al., 1998; Yonei-Tamura et al., 1999; Takabatake et al., 2000; Tümpel et al., 2002).

In *S. canicula*, *Tbx3* is not expressed in lateral line placodes at any stage; however, it is expressed in the otic placode, and in developing vestibuloacoustic and lateral line ganglia. Later, it is also expressed in the trigeminal ganglion, as was similarly reported in the mouse at late stages (Chapman et al., 1996). A detailed description follows below.

We detected no *Tbx3* expression at stage 18 (18-22 days; data not shown). By stage 21 (26-27 days; Fig. 9A,B), *Tbx3* is expressed strongly in the developing otic placode, and in the vestibuloacoustic/anterodorsal lateral line ganglionic complex located rostral to it (compare with *NeuroD* expression at the same stage; Fig. 9C). *Tbx3* is also expressed in the dorsal retina, in the branchial arches, in the anterior lateral plate mesoderm, in the proctodeum, and in the notochord posterior to the proctodeum.

At stage 23 (28-30 days; Fig. 9D,E), *Tbx3* expression is maintained in the vestibuloacoustic and anterodorsal lateral line ganglia. Faint expression is also seen in separate patches dorsal to the third and fourth branchial arches, with a more extended patch lying dorsal to the fifth and sixth branchial arches. A comparison with *NeuroD* expression at the same stage (Fig. 9F) suggests that this represents expression in the three post-otic lateral line ganglia (middle, supratemporal and posterior). Sections (not shown; see Fig. 10) confirm that *Tbx3* is expressed in ganglia rather than in placodes. Additional expression is seen faintly in the pineal gland and in hypaxial muscle primordia.

At stage 25 (31-38 days; Fig 9G), *Tbx3* expression is stronger in all these domains. A small patch of expression just ventral to the anterodorsal lateral line ganglion probably represents the anteroventral lateral line ganglion. *Tbx3* expression in the three post-otic lateral line ganglia is stronger at this stage and can be compared both with *NeuroD* expression (Fig. 9H)

and, by double *in situ* hybridisation, with *Eya4* expression in lateral line placodes (Fig. 9I). The *Tbx3*$^{+}$ post-otic lateral line ganglia are overlain by *Eya4*$^{+}$ lateral line placodes; the posterior lateral line ganglion is overlain by the trailing edge of the *Eya4*$^{+}$ posterior lateral line primordium, which has already begun migrating onto the trunk in this embryo (Fig. 9I). A small patch of *Tbx3* expression is also seen at the dorsal edge of the olfactory pits (Fig. 9G). In sections (not shown; also see Fig. 10H), this patch of expression is seen to be in the mesenchyme, not the olfactory epithelium.

At stage 26 (37-42 days; Fig. 9J,K) and stage 27 (42-46 days; Fig. 9L-N), *Tbx3* expression is maintained in the anterodorsal and anteroventral lateral line ganglia as well as the three post-otic lateral line ganglia (middle, supratemporal and posterior) and at least part of the vestibuloacoustic ganglion. The anteroventral lateral line ganglion is more clearly visible at stage 27 (Fig. 9M,N), located ventral to the anterodorsal lateral line ganglion and just dorsal to the position of the geniculate ganglion (compare with *NeuroD* expression; Fig. 9O). Although at earlier stages, the vestibuloacoustic ganglion as visualised by both *NeuroD* and *Tbx3* expression seemed to abut the rostral edge of the otic vesicle (e.g. Fig. 9G,H), by stage 27 the expression of both genes seems to be missing from the region immediately rostral to the otic vesicle, apart from a thin stripe of *Tbx3* expression (Fig. 9M,N). This stripe may represent the subset of vestibuloacoustic ganglion cells that is seen in sections to maintain *Tbx3* expression at stage 28 (Fig. 10I,J). Also at stage 27, *Tbx3* expression is seen in what appears to be the trigeminal ganglion (Fig. 9M), although this can be obscured in wholemount by the rostral spur of the anterodorsal lateral line ganglion (as in Fig. 9N). *Tbx3* is also expressed in the pectoral fin bud and in the median fin fold, though not in the future dorsal and anal fin regions (Fig. 9J and data not shown).

At stage 28 (46-51 days; Fig. 10A,B,E-R), and also at stage 29 (49-53 days; Fig. 10C), *Tbx3* expression is still evident in the anterodorsal and posterior lateral line ganglia in wholemount (compare with neurofilament staining at stage 28; Fig. 10D). *In situ* hybridisation on sections at stage 28 confirms expression in these ganglia (not shown) but also demonstrates *Tbx3* expression in a subset of trigeminal ganglion cells (Fig. 10E-G), and in a small number of vestibuloacoustic ganglion cells (Fig. 10I,J). *In situ* hybridisation on sections at stage 28 also showed *Tbx3* expression in the middle (not shown) and supratemporal lateral line ganglia (Fig. 10N-R). We did not see convincing *Tbx3* expression above background in the epibranchial placode-derived ganglia, however (Fig. 10N-R). Thus, by stage 28, while *Tbx3* is no longer absolutely specific for the lateral line ganglia, it still appears to distinguish between lateral line and epibranchial placode-derived ganglia. *In situ* hybridisation on sections also confirms *Tbx3* expression in the pineal gland (not shown; see Fig. 9A-C), neurohypophysis (Fig. 10E,F), dorsal retina (Fig. 10E-G), specific regions of the otic vesicle (possibly sensory patches; Fig. 10C,I-L), in mesenchyme adjacent to the olfactory pits (Fig. 10H), in the periphery of the mandibular arch (Fig. 10K,M), and in the external gill filaments (Fig. 10N,P).

Overall, therefore, *Tbx3* is a novel marker for lateral line and vestibuloacoustic ganglia in shark embryos, as well as (at later stages) a subset of trigeminal neurons.

Europe PMC Funders Author Manuscripts

Discussion

Cranial placodes were first described in shark embryos (van Wijhe, 1882), but until now, nothing was known about the development of shark placodes at the molecular level. Many genes known to be important for placode development in amniotes and amphibians are conserved in teleosts (reviewed in Baker and Bronner-Fraser, 2001; Schlosser, 2006), and the expression of two *Pax* genes had been shown to be conserved in lamprey placodes (McCauley and Bronner-Fraser, 2002). Hence, pan-vertebrate conservation of the genetic networks controlling placode development seemed likely, but had not been tested in the most basal extant gnathostome clade, the chondrichthyans. We cloned and analysed the spatiotemporal expression pattern of six transcription factors (*NeuroD*, *Pax3*, *Pax2*, *Phox2b*, *Eya4* and *Tbx3*) likely to be expressed in different placodes and placode-derived neurons in the lesser-spotted dogfish/catshark, *Scyliorhinus canicula*. We used the spatiotemporal expression pattern of these genes to characterise the development of cranial placodes and their associated sensory ganglia in *S. canicula*. Our findings demonstrate the evolutionary conservation across all vertebrates of at least some of the transcription factor networks underlying cranial neurogenic placode development. They provide strong support for the homology of the profundal placode of elasmobranchs and basal actinopterygians and the amniote ophthalmic trigeminal (opV) placode. We have also identifed *Eya4* as a novel marker for the lateral line system throughout its development, and *Tbx3* as a specific marker for lateral line placode-derived ganglia.

Pax3 expression in the shark profundal placode strongly supports its homology with the amniote ophthalmic trigeminal placode

In amniotes, the trigeminal ganglion is a bi-lobed structure with two main divisions: ophthalmic (opV) and maxillomandibular (mmV). The neurons in the distal region of each ganglionic lobe are derived from opV and mmV placodes, respectively, while the neurons in the proximal region are derived from neural crest cells, as are all satellite glial cells within the ganglion (Hamburger, 1961; D'Amico-Martel and Noden, 1983). Trigeminal neural crest cells arrive at the site of ganglion formation first (Covell and Noden, 1989), but differentiate much later than opV and mmV placode-derived cells (D'Amico-Martel and Noden, 1980; D'Amico-Martel, 1982). Trigeminal neural crest cells are not required for the formation of placode-derived neurons, nor for target finding in the periphery (Hamburger, 1961; Moody and Heaton, 1983; Stark et al., 1997) although there is a delay in the formation of the central projections of placode-derived neurons when neural crest cells are ablated (Moody and Heaton, 1983). Importantly, separate opV and mmV placode-derived ganglia form in the absence of neural crest cells, suggesting that neural crest cells act as an aggregation centre for placode-derived neurons, enabling a fused bi-lobed ganglion to form (Hamburger, 1961).

In elasmobranchs and basal actinopterygians, however, two completely separate somatosensory cranial ganglia are found: the profundal and trigeminal ganglia. In lamprey and amphibian embryos, two separate ganglia form initially, but these fuse either during development or (in frogs) are fused proximally from the start (Northcutt and Brändle, 1995; Schlosser and Roth, 1997; Kuratani et al., 1997). It has been controversial whether or not the profundal placode and profundal placode-derived ganglion of anamniotes are homologous to

the opV placode and opV placode-derived opV neurons of amniotes (Northcutt and Brändle, 1995). In chick embryos, the opV placode and opV placode-derived neurons express Pax3 (Stark et al., 1997; Baker et al., 2002). Similarly, in *Xenopus*, the profundal/opV placode and ganglion express *Pax3* (Schlosser and Ahrens, 2004). We have shown here that *Pax3* is expressed in the profundal placode and profundal placode-derived cells in sharks. Our results, therefore, strongly support the homology of the profundal placode of elasmobranchs and basal actinopterygians, the profundal/opV placode of amphibians, and the amniote opV placode.

Evolution of vertebrate *Pax3/7* genes

Only a single *Pax3/7* gene has so far been described in each of two different lamprey species, *Petromyzon marinus* (McCauley and Bronner-Fraser, 2002) and *Lampetra fluviatilis* (Osorio et al., 2005). The *Petromyzon* gene was reported to be orthologous to gnathostome *Pax7* genes (McCauley and Bronner-Fraser, 2002), while the orthology of the *Lampetra Pax3/7* gene, though 97% identical at the amino acid level to the predicted *Petromyzon* Pax7 protein, was unresolved (Osorio et al., 2005). Including *S. canicula Pax3* in the phylogenetic analysis (Fig. 1B) yields a topology with strong support for the hypothesis that both lamprey genes are orthologous to gnathostome *Pax7* genes. The single amphioxus and ascidian *Pax3/7* genes, in contrast, group together outside all vertebrate *Pax3* and *Pax7* genes (Fig. 1B). These results suggest either that a lamprey *Pax3* gene remains to be discovered, or that it has been lost in both lamprey species, or that lampreys have a single *Pax3/7* gene that is more *Pax7*-like in sequence than the single invertebrate chordate *Pax3/7* gene. Isolation of *Pax3/7* genes from hagfishes would be very informative in this regard.

Pax2 is a conserved pan-gnathostome marker for both otic and epibranchial placodes

The paired domain transcription factor Pax2 is an early molecular marker for the otic placodes of all vertebrates, including lampreys (McCauley and Bronner-Fraser, 2002) and, as we have confirmed here, sharks. The cochlea fails to form in *Pax2*-deficient mice (Torres et al., 1996), demonstrating the importance of *Pax2* for later otic patterning and morphogenesis. However, mutant and morphant analyses in zebrafish have shown that *Pax2* is also important for otic placode formation: here, it acts in a synergistic and partially redundant fashion with its close relative, *Pax8*, which is expressed earlier than *Pax2* in the prospective otic region (Hans et al., 2004; Mackereth et al., 2005). The model proposed is that *Pax8* is required to initiate otic placode formation, while *Pax2* is required to maintain subsequent development (Hans et al., 2004; Mackereth et al., 2005).

We observed that expression of *Pax2* within the dogfish otic placode is gradually restricted dorso-medially in a manner analogous to that seen in the chick embryo (Hidalgo-Sánchez et al., 2000). At later stages, *Pax2* expression is seen in presumptive sensory patches and hair cells. This implies that some of the basic mechanisms of otic patterning are well conserved among gnathostomes, thus *Pax2* may be similarly involved in otic specification and compartmentalization in sharks. It remains to be determined whether other molecules implicated in patterning the otocyst (reviewed in Barald and Kelley, 2004) are similarly conserved.

Neither *Pax2* expression, nor a combination of *Pax8* and *Pax2* expression, is sufficient to specify an otic fate. Neither gene is an exclusive marker for the otic placodes: *Pax2*, at least, is also expressed in the epibranchial placodes in chick, mouse and *Xenopus* (Baker and Bronner-Fraser, 2000; Ohyama and Groves, 2004; Schlosser and Ahrens, 2004). In *Xenopus*, both *Pax2* and *Pax8* are expressed in the common thickened dorsolateral placode area from which the otic, lateral line and epibranchial placodes arise (Schlosser and Ahrens, 2004). *Pax2* is maintained in otic and epibranchial placodes but downregulated in lateral line placodes, while *Pax8* is downregulated first in epibranchial placodes and later in lateral line placodes (Schlosser and Ahrens, 2004). Fatemapping experiments in the chick have shown that cells within the early broad ectodermal expression domain of *Pax2* contribute not only to the otic placodes, but also to the epibranchial placodes and to epidermis (Streit, 2002). Recent studies using a *Pax2*-Cre mouse line have demonstrated that *Pax2*$^{+}$ cells that receive a Wnt signal adopt an otic placode fate, while *Pax2*$^{+}$ cells that do not receive a Wnt signal adopt an epidermal fate (Ohyama et al., 2006). It is not yet clear in any species how the epibranchial placode domain of *Pax2* expression is induced or maintained, or what might be the role of *Pax2* in the epibranchial placodes. Nonetheless, we have shown here that *Pax2* is a conserved pan-gnathostome marker for the epibranchial placodes, suggesting that *Pax2* must be important for some aspect of their development. It may well be that, as for otic placode development, *Pax2* and *Pax8* act redundantly in epibranchial placode development; however, this awaits further investigation.

Phox2b is a conserved pan-gnathostome marker for epibranchial placode-derived neurons

Phox2b is a homeodomain transcription factor essential for the development of the autonomic nervous system, where it is a key determinant of the noradrenergic phenotype (reviewed in Brunet and Pattyn, 2002). It is also expressed in all epibranchial placode-derived neurons in the geniculate, petrosal and nodose ganglia: as well as innervating taste buds (not yet experimentally proven, but see Gross et al., 2003; Northcutt, 2004), these *Phox2b*$^{+}$ neurons make up the afferent arm of medullary reflex circuits controlling autonomic (visceral) functions (reviewed in Brunet and Pattyn, 2002). In the mouse, the closely related transcription factor *Phox2a* is expressed before *Phox2b* in epibranchial placode-derived neuroblasts; in the absence of either gene, the epibranchial placode-derived ganglia form but subsequently degenerate, though the atrophy is more complete in *Phox2b*$^{-/-}$ mice (Pattyn et al., 1999; Dauger et al., 2003). *Phox2b*$^{+}$ neurons have different embryonic origins (neural tube, neural crest, epibranchial placodes), positions and neurotransmitter phenotypes; the main feature uniting them seems to be their involvement in visceral reflex circuits, in which *Phox2b*$^{+}$ neurons connect with other *Phox2b*$^{+}$ neurons (reviewed in Brunet and Pattyn, 2002; also see Dauger et al., 2003). Therefore, Phox2b seems to act as a visceral reflex circuit-specific transcription factor. The association of *Phox2* genes with control of visceral function predates vertebrate origins: the muscles that control closure or contraction of the adult ascidian pharynx, and the surrounding atrium, are innervated by *Phox2*$^{+}$ motor neurons in the cerebral ganglion (Dufour et al., 2006). We have shown here that *Phox2b* is expressed in epibranchial placode-derived neurons in shark embryos, therefore is a pan-gnathostome marker for these neurons. The only vertebrate sensory neurons known to express *Phox2* genes are epibranchial placode-derived neurons. From the perspective of vertebrate placode evolution, therefore, it would be fascinating to learn whether or not any

sensory neurons in either ascidians or amphioxus express *Phox2* genes, and if so, their position, function and embryonic origin.

Eya4 is a novel marker for the lateral line system throughout its development

We cloned *S. canicula Eya4* in an attempt to isolate *Eya1* as a pan-placodal marker. There are four vertebrate homologues of the *Drosophila eyes-absent* (*eya*) gene, encoding the transcription co-factors/protein tyrosine phosphatases Eya1-4 (reviewed in Rebay et al., 2005). *Eya1* (in *Xenopus*) and *Eya2* (in chick and zebrafish) can be considered as pan-placodal markers: they are expressed in the preplacodal region and subsequently maintained in individual placodes (reviewed in Bailey and Streit, 2006; Schlosser, 2006). Mutations in *Eya1* cause deafness (amongst other defects) in human branchio-oto-renal syndrome; inner ear and cranial sensory ganglion deficiencies in mice; and inner ear and lateral line deficiencies in zebrafish (reviewed in Rebay et al., 2005). Vertebrate *Eya* genes have non-placodal functions as well, however: for example, in the chick, *Eya2*, *Six1*, *Dach2* and *Pax3* genes interact in a complex synergistic network to regulate myogenesis (Heanue et al., 1999).

We found shark *Eya4* to be expressed in the otic vesicle, as previously reported for mouse and rat (Borsani et al., 1999; Wayne et al., 2001). In the rat, *Eya4* expression in the developing inner ear is localised to the cochlear duct and the sensory epithelia of the vestibular system (Wayne et al., 2001). We also found *Eya4* to be a novel marker for the shark lateral line system throughout its development, from placodes to differentiating neuromasts (confined to a few cells, probably hair cells) and electroreceptive ampullary organs. In zebrafish, the *eya4* expression pattern was analysed briefly and expression in the somites and lateral line neuromasts mentioned, but expression in lateral line placodes and migrating primordia was not described (Schönberger et al., 2005). Mutations in *Eya4* cause late-onset sensorineural hearing loss in humans (Wayne et al., 2001; Pfister et al., 2002; Schönberger et al., 2005), consistent with a role for *Eya4* in hair cells, at least in the inner ear. The function of *Eya4* in the development of the lateral line system awaits further analysis.

Eya4 expression in shark ampullary organs (electroreceptors) as well as neuromasts should serve as a useful marker for future studies on the development of electroreceptors, which are very little understood. Although a recent report suggested that *S. canicula* electroreceptors develop from neural crest cells (Freitas et al., 2006), this was based on the expression in ampullary organs of *Sox8*, and of an antigen recognised by the HNK1 antibody, neither of which is a specific marker for neural crest cells. HNK1 recognises a carbohydrate epitope found on many proteins; it is not specific for neural crest cells in any vertebrate embryo, and it does not recognise neural crest cells in mice, amphibians, or the closely related shark *Scyliorhinus torazame* (Tucker et al., 1988; Kuratani and Horigome, 2000). Furthermore, ablation and grafting experiments in the axolotl have shown that individual lateral line placodes give rise both to neuromasts and ampullary organs (Northcutt et al., 1995). The current model for electroreceptor development is that the sensory ridge formed by the elongation of each lateral line placode on the head is polarised into a central zone that forms neuromasts, and lateral flanking zones that form electroreceptors (Northcutt et al., 1994,

1995). The development in *S. canicula* embryos of *Eya4*$^{+}$ ampullary organs in zones flanking lines of *Eya4*$^{+}$ neuromasts, along the elongation path of *Eya4*$^{+}$ lateral line placode-derived sensory ridges, would seem to provide support for this model.

Tbx3 is expressed in lateral line and vestibuloacoustic ganglia in shark embryos

The T-box transcription factor Tbx3 is best known for its role in limb development, where it is important for patterning the posterior digits (reviewed in Naiche et al., 2005; King et al., 2006). Haploinsufficiency for *Tbx3* causes ulnar-mammary syndrome in humans, in which the mammary glands are hypoplastic, the external genitalia are abnormal, and there are posterior forelimb defects involving the ulna and little finger (Bamshad et al., 1997). Homozygous *Tbx3* mutations in mice are embryonic lethal due to yolk sac defects; they have mammary gland and mild defects in posterior elements of the fore- and hindlimbs (Davenport et al., 2003). *Tbx3* is expressed along the anterior and posterior edges of the limb buds: mis-expression studies in chick embryos have confirmed that *Tbx3* is a key determinant of posterior digit identity (Suzuki et al., 2004), and also shown that *Tbx3* helps to determine the position of the limb along the main body axis (Rallis et al., 2005).

We cloned *S. canicula Tbx3* as a putative lateral line placode marker, based on reported expression patterns in *Xenopus* (Li et al., 1997; Takabatake et al., 2000; Schlosser and Ahrens, 2004). We found that although *Tbx3* is expressed in the otic placode, it is not expressed in lateral line placodes at any stage; however, it is expressed in lateral line (and vestibuloacoustic) ganglia. Given our results, the reported expression of *Tbx3* in "cranial ganglia" in *Xenopus* (Li et al., 1997; Takabatake et al., 2000), which was subsequently suggested to be lateral line placode-specific expression (Schlosser and Ahrens, 2004), seems more likely to represent lateral line ganglia, though this needs to be confirmed. Since in many anamniotes, including *S. canicula*, lateral line ganglia are often found in very close contact with epibranchial placode-derived ganglia, *Tbx3* should serve as a useful marker for lateral line placode-derived elements in such compound ganglia. At later stages, *Tbx3* is also expressed in a subset of trigeminal neurons, and also maintained in a small subset of neurons in the vestibuloacoustic ganglion.

The role of *Tbx3* in cranial sensory neurons remains to be determined. In zebrafish, *tbx2b* (formerly *tbx-c*) has a similar expression pattern to *S. canicula Tbx3*, including in the trigeminal and lateral line ganglia (Dheen et al., 1999). *Tbx2* and *Tbx3* evolved by gene duplication (Agulnik et al., 1996; Ruvinsky and Gibson-Brown, 2000) and are expressed in overlapping but distinct patterns (e.g. Chapman et al., 1996; Gibson-Brown et al., 1998). Transplantation experiments using *tbx2b*-morphant cells have suggested a role for *tbx2b* in both cell movement and neuronal differentiation (Fong et al., 2005), while neuronal differentiation in the dorsal retina is blocked in *tbx2b*-morphant embryos (Gross and Dowling, 2005). It seems likely, therefore, that *Tbx3* is also involved in some aspect of neuronal differentiation in lateral line, vestibuloacoustic and trigeminal ganglia, but this awaits further investigation.

Summary

We have undertaken the first molecular analysis of neurogenic placode and cranial sensory ganglion development in shark embryos. We have found that *S. canicula Pax3* is expressed in the profundal placode, providing strong support for its homology with the amniote ophthalmic trigeminal placode. We have shown that *Pax2* and *Phox2b* are conserved pan-gnathostome markers for epibranchial placodes and epibranchial placode-derived neurons, respectively, and we have confirmed pan-vertebrate conservation of *Pax2* expression in the otic placode. We have identified *Eya4* as a novel marker for the lateral line system throughout its development, from placodes to differentiating neuromasts and electroreceptive ampullary organs. Finally, we have shown that *Tbx3* is a specific marker (at least initially) for lateral line ganglia. Overall, our results support a high degree of conservation across all gnathostomes of the transcription factor networks underlying neurogenic placode and cranial sensory ganglion development.

Supplementary Material

Refer to Web version on PubMed Central for supplementary material.

Acknowledgments

Thanks to Dr Sylvie Mazan, Dr Martin Cohn, Renata Freitas, Dr Jean-François Brunet and Professor Glenn Northcutt for invaluable advice and protocols, and to two anonymous reviewers for very helpful comments. Thanks to Dr David Sims and Victoria Wearmouth (Marine Biological Association of the UK, Plymouth), and to the University of Glasgow's Marine Biological Station (Millport), for supplying embryos. This work was supported by BBSRC grants G18657 and BB/D008336/1 to C.V.H.B.

References

Agulnik SI, Garvey N, Hancock S, Ruvinsky I, Chapman DL, Agulnik I, Bollag R, Papaioannou V, Silver LM. Evolution of mouse T-box genes by tandem duplication and cluster dispersion. Genetics. 1996; 144:249–254. [PubMed: 8878690]

Bailey AP, Streit A. Sensory organs: making and breaking the pre-placodal region. Curr Top Dev Biol. 2006; 72:167–204. [PubMed: 16564335]

Baker CVH, Bronner-Fraser M. The origins of the neural crest. Part II: an evolutionary perspective. Mech Dev. 1997; 69:13–29. [PubMed: 9486528]

Baker CVH, Bronner-Fraser M. Establishing neuronal identity in vertebrate neurogenic placodes. Development. 2000; 127:3045–3056. [PubMed: 10862742]

Baker CVH, Bronner-Fraser M. Vertebrate cranial placodes I. Embryonic induction. Dev Biol. 2001; 232:1–61. [PubMed: 11254347]

Baker CVH, Schlosser G. Editorial: The evolutionary origin of neural crest and placodes. J Exp Zool B Mol Dev Evol. 2005; 304:269–273. [PubMed: 16003767]

Baker CVH, Stark MR, Bronner-Fraser M. Pax3-expressing trigeminal placode cells can localize to trunk neural crest sites but are committed to a cutaneous sensory neuron fate. Dev Biol. 2002; 249:219–236. [PubMed: 12221003]

Ballard WW, Mellinger J, Lechenault H. A series of normal stages for development of *Scyliorhinus canicula*, the lesser spotted dogfish (*Chondrichthyes*: *Scylorhinidae*). J Exp Zool. 1993; 267:318–336.

Bamshad M, Lin RC, Law DJ, Watkins WC, Krakowiak PA, Moore ME, Franceschini P, Lala R, Holmes LB, Gebuhr TC, Bruneau BG, et al. Mutations in human *TBX3* alter limb, apocrine and genital development in ulnar-mammary syndrome. Nat Genet. 1997; 16:311–315. [PubMed: 9207801]

Barald KF, Kelley MW. From placode to polarization: new tunes in inner ear development. Development. 2004; 131:4119–4130. [PubMed: 15319325]

Bhattacharyya S, Bailey AP, Bronner-Fraser M, Streit A. Segregation of lens and olfactory precursors from a common territory: cell sorting and reciprocity of Dlx5 and Pax6 expression. Dev Biol. 2004; 271:403–414. [PubMed: 15223343]

Borsani G, DeGrandi A, Ballabio A, Bulfone A, Bernard L, Banfi S, Gattuso C, Mariani M, Dixon M, Donnai D, Metcalfe K, et al. EYA4, a novel vertebrate gene related to *Drosophila eyes absent*. Hum Mol Genet. 1999; 8:11–23. [PubMed: 9887327]

Brunet JF, Pattyn A. *Phox2* genes - from patterning to connectivity. Curr Opin Genet Dev. 2002; 12:435–440. [PubMed: 12100889]

Burrill JD, Moran L, Goulding MD, Saueressig H. PAX2 is expressed in multiple spinal cord interneurons, including a population of EN1+ interneurons that require PAX6 for their development. Development. 1997; 124:4493–4503. [PubMed: 9409667]

Chae JH, Stein GH, Lee JE. NeuroD: the predicted and the surprising. Mol Cells. 2004; 18:271–288. [PubMed: 15650322]

Chapman DL, Garvey N, Hancock S, Alexiou M, Agulnik SI, Gibson-Brown JJ, Cebra-Thomas J, Bollag RJ, Silver LM, Papaioannou VE. Expression of the T-box family genes, *Tbx1-Tbx5* during early mouse development. Dev Dyn. 1996; 206:379–390. [PubMed: 8853987]

Chi N, Epstein JA. Getting your Pax straight: Pax proteins in development and disease. Trends Genet. 2002; 18:41–47. [PubMed: 11750700]

Covell DA Jr, Noden DM. Embryonic development of the chick primary trigeminal sensory-motor complex. J Comp Neurol. 1989; 286:488–503. [PubMed: 2778103]

D'Amico-Martel A. Temporal patterns of neurogenesis in avian cranial sensory and autonomic ganglia. Am J Anat. 1982; 163:351–372. [PubMed: 7091019]

D'Amico-Martel A, Noden DM. An autoradiographic analysis of the development of the chick trigeminal ganglion. J Embryol Exp Morphol. 1980; 55:167–182. [PubMed: 6966308]

D'Amico-Martel A, Noden DM. Contributions of placodal and neural crest cells to avian cranial peripheral ganglia. Am J Anat. 1983; 166:445–468. [PubMed: 6858941]

Dauger S, Pattyn A, Lofaso F, Gaultier C, Goridis C, Gallego J, Brunet J-F. *Phox2b* controls the development of peripheral chemoreceptors and afferent visceral pathways. Development. 2003; 130:6635–6642. [PubMed: 14627719]

Davenport TG, Jerome-Majewska LA, Papaioannou VE. Mammary gland, limb and yolk sac defects in mice lacking *Tbx3*, the gene mutated in human ulnar mammary syndrome. Development. 2003; 130:2263–2273. [PubMed: 12668638]

David NB, Sapède D, Saint-Etienne L, Thisse C, Thisse B, Dambly-Chaudière C, Rosa FM, Ghysen A. Molecular basis of cell migration in the fish lateral line: role of the chemokine receptor CXCR4 and of its ligand, SDF1. Proc Natl Acad Sci USA. 2002; 99:16297–16302. [PubMed: 12444253]

Dheen T, Sleptsova-Friedrich I, Xu Y, Clark M, Lehrach H, Gong Z, Korzh V. Zebrafish *tbx-c* functions during formation of midline structures. Development. 1999; 126:2703–2713. [PubMed: 10331981]

Dufour HD, Chettouh Z, Deyts C, de Rosa R, Goridis C, Joly J-S, Brunet J-F. Precraniate origin of cranial motoneurons. Proc Natl Acad Sci USA. 2006

Firnberg N, Neubüser A. FGF signaling regulates expression of *Tbx2*, *Erm*, *Pea3*, and *Pax3* in the early nasal region. Dev Biol. 2002; 247:237–250. [PubMed: 12086464]

Fong SH, Emelyanov A, Teh C, Korzh V. Wnt signalling mediated by Tbx2b regulates cell migration during formation of the neural plate. Development. 2005; 132:3587–3596. [PubMed: 16033799]

Freitas R, Cohn MJ. Analysis of *EphA4* in the lesser spotted catshark identifies a primitive gnathostome expression pattern and reveals co-option during evolution of shark-specific morphology. Dev Genes Evol. 2004; 214:466–472. [PubMed: 15300436]

Freitas R, Zhang G, Albert JS, Evans DH, Cohn MJ. Developmental origin of shark electrosensory organs. Evol Dev. 2006; 8:74–80. [PubMed: 16409384]

Gans C, Northcutt RG. Neural crest and the origin of vertebrates: a new head. Science. 1983; 220:268–274. [PubMed: 17732898]

Gibbs MA, Northcutt RG. Development of the lateral line system in the shovelnose sturgeon. Brain Behav Evol. 2004; 64:70–84. [PubMed: 15205543]

Gibson-Brown JJ, Agulnik SI, Silver LM, Papaioannou VE. Expression of T-box genes *Tbx2-Tbx5* during chick organogenesis. Mech Dev. 1998; 74:165–169. [PubMed: 9651516]

Goulding MD, Chalepakis G, Deutsch U, Erselius JR, Gruss P. Pax-3, a novel murine DNA binding protein expressed during early neurogenesis. EMBO J. 1991; 10:1135–1147. [PubMed: 2022185]

Graham A, Begbie J. Neurogenic placodes: a common front. Trends Neurosci. 2000; 23:313–316. [PubMed: 10856941]

Gross JB, Gottlieb AA, Barlow LA. Gustatory neurons derived from epibranchial placodes are attracted to, and trophically supported by, taste bud-bearing endoderm in vitro. Dev Biol. 2003; 264:467–481. [PubMed: 14651931]

Gross JM, Dowling JE. *Tbx2b* is essential for neuronal differentiation along the dorsal/ventral axis of the zebrafish retina. Proc Natl Acad Sci USA. 2005; 102:4371–4376. [PubMed: 15755805]

Haas P, Gilmour D. Chemokine signaling mediates self-organizing tissue migration in the zebrafish lateral line. Dev Cell. 2006; 10:673–680. [PubMed: 16678780]

Hamburger V. Experimental analysis of the dual origin of the trigeminal ganglion in the chick embryo. J Exp Zool. 1961; 148:91–117. [PubMed: 13904079]

Hans S, Liu D, Westerfield M. Pax8 and Pax2a function synergistically in otic specification, downstream of the Foxi1 and Dlx3b transcription factors. Development. 2004; 131:5091–5102. [PubMed: 15459102]

Heanue TA, Reshef R, Davis RJ, Mardon G, Oliver G, Tomarev S, Lassar AB, Tabin CJ. Synergistic regulation of vertebrate muscle development by *Dach2*, *Eya2*, and *Six1*, homologs of genes required for *Drosophila* eye formation. Genes Dev. 1999; 13:3231–3243. [PubMed: 10617572]

Hidalgo-Sánchez M, Alvarado-Mallart R, Alvarez IS. *Pax2*, *Otx2*, *Gbx2* and *Fgf8* expression in early otic vesicle development. Mech Dev. 2000; 95:225–229. [PubMed: 10906468]

Johnson SE. Structure and development of the sense organs of the lateral canal system of Selachians (*Mustelus canis* and *Squalus acanthias*). J Comp Neur. 1917; 28:1–74.

King M, Arnold JS, Shanske A, Morrow BE. T-genes and limb bud development. Am J Med Genet A. 2006; 140:1407–1413. [PubMed: 16688725]

Kuratani S, Horigome N. Developmental morphology of branchiomeric nerves in a cat shark, *Scyliorhinus torazame*, with special reference to rhombomeres, cephalic mesoderm, and distribution patterns of cephalic crest cells. Zool Sci. 2000; 17:893–909.

Kuratani S, Ueki T, Aizawa S, Hirano S. Peripheral development of cranial nerves in a cyclostome, *Lampetra japonica*: morphological distribution of nerve branches and the vertebrate body plan. J Comp Neurol. 1997; 384:483–500. [PubMed: 9259485]

Landacre FL. The cerebral ganglia and early nerves of *Squalus acanthias*. J Comp Neur. 1916; 27:19–67.

Li H, Tierney C, Wen L, Wu JY, Rao Y. A single morphogenetic field gives rise to two retina primordia under the influence of the prechordal plate. Development. 1997; 124:603–615. [PubMed: 9043075]

Mackereth MD, Kwak SJ, Fritz A, Riley BB. Zebrafish *pax8* is required for otic placode induction and plays a redundant role with Pax2 genes in the maintenance of the otic placode. Development. 2005; 132:371–382. [PubMed: 15604103]

Martin K, Groves AK. Competence of cranial ectoderm to respond to Fgf signaling suggests a two-step model of otic placode induction. Development. 2006; 133:877–887. [PubMed: 16452090]

McCauley DW, Bronner-Fraser M. Conservation of *Pax* gene expression in ectodermal placodes of the lamprey. Gene. 2002; 287:129–139. [PubMed: 11992731]

Moody SA, Heaton MB. Developmental relationships between trigeminal ganglia and trigeminal motoneurons in chick embryos. II. Ganglion axon ingrowth guides motoneuron migration. J Comp Neurol. 1983; 213:344–349. [PubMed: 6601117]

Naiche LA, Harrelson Z, Kelly RG, Papaioannou VE. T-box genes in vertebrate development. Annu Rev Genet. 2005; 39:219–239. [PubMed: 16285859]

Norris HW, Hughes SP. The cranial, occipital, and anterior spinal nerves of the dogfish, *Squalus acanthias* . J Comp Neurol. 1920; 31:293–402.

Northcutt RG. Evolution of gnathostome lateral line ontogenies. Brain Behav Evol. 1997; 50:25–37. [PubMed: 9209764]

Northcutt RG. Taste buds: development and evolution. Brain Behav Evol. 2004; 64:198–206. [PubMed: 15353910]

Northcutt RG. The New Head hypothesis revisited. J Exp Zool B Mol Dev Evol. 2005; 304B:274–297.

Northcutt RG, Brändle K. Development of branchiomeric and lateral line nerves in the axolotl. J Comp Neurol. 1995; 355:427–454. [PubMed: 7636024]

Northcutt RG, Brändle K, Fritzsch B. Electroreceptors and mechanosensory lateral line organs arise from single placodes in axolotls. Dev Biol. 1995; 168:358–373. [PubMed: 7729575]

Northcutt RG, Catania KC, Criley BB. Development of lateral line organs in the axolotl. J Comp Neurol. 1994; 340:480–514. [PubMed: 8006214]

Northcutt RG, Gans C. The genesis of neural crest and epidermal placodes: a reinterpretation of vertebrate origins. Quart Rev Biol. 1983; 58:1–28. [PubMed: 6346380]

Ohyama T, Groves AK. Generation of Pax2-Cre mice by modification of a Pax2 bacterial artificial chromosome. Genesis. 2004; 38:195–199. [PubMed: 15083520]

Ohyama T, Mohamed OA, Taketo MM, Dufort D, Groves AK. Wnt signals mediate a fate decision between otic placode and epidermis. Development. 2006; 133:865–875. [PubMed: 16452098]

Osorio J, Mazan S, Rétaux S. Organisation of the lamprey (*Lampetra fluviatilis*) embryonic brain: insights from LIM-homeodomain, Pax and hedgehog genes. Dev Biol. 2005; 288:100–112. [PubMed: 16289025]

Pattyn A, Morin X, Cremer H, Goridis C, Brunet JF. The homeobox gene *Phox2b* is essential for the development of autonomic neural crest derivatives. Nature. 1999; 399:366–370. [PubMed: 10360575]

Pfister M, Toth T, Thiele H, Haack B, Blin N, Zenner HP, Sziklai I, Nurnberg P, Kupka S. A 4-bp insertion in the eya-homologous region (eyaHR) of EYA4 causes hearing impairment in a Hungarian family linked to DFNA10. Mol Med. 2002; 8:607–611. [PubMed: 12477971]

Rallis C, Del Buono J, Logan MPO. *Tbx3* can alter limb position along the rostrocaudal axis of the developing embryo. Development. 2005; 132:1961–1970. [PubMed: 15790970]

Rebay I, Silver SJ, Tootle TL. New vision from Eyes absent: transcription factors as enzymes. Trends Genet. 2005; 21:163–171. [PubMed: 15734575]

Relaix F, Polimeni M, Rocancourt D, Ponzetto C, Schafer BW, Buckingham M. The transcriptional activator PAX3-FKHR rescues the defects of Pax3 mutant mice but induces a myogenic gain-of-function phenotype with ligand-independent activation of Met signaling in vivo. Genes Dev. 2003; 17:2950–2965. [PubMed: 14665670]

Rose TM, Henikoff JG, Henikoff S. CODEHOP (COnsensus-DEgenerate Hybrid Oligonucleotide Primer) PCR primer design. Nucleic Acids Res. 2003; 31:3763–3766. [PubMed: 12824413]

Ruvinsky I, Gibson-Brown JJ. Genetic and developmental bases of serial homology in vertebrate limb evolution. Development. 2000; 127:5233–5244. [PubMed: 11076746]

Schlosser G. Evolutionary origins of vertebrate placodes: insights from developmental studies and from comparisons with other deuterostomes. J Exp Zoolog B Mol Dev Evol. 2005; 304:347–399.

Schlosser G. Induction and specification of cranial placodes. Dev Biol. 2006; 294:303–351. [PubMed: 16677629]

Schlosser G, Ahrens K. Molecular anatomy of placode development in *Xenopus laevis*. Dev Biol. 2004; 271:439–466. [PubMed: 15223346]

Schlosser G, Northcutt RG. Development of neurogenic placodes in *Xenopus laevis*. J Comp Neurol. 2000; 418:121–146. [PubMed: 10701439]

Schlosser G, Roth G. Evolution of nerve development in frogs. I. The development of the peripheral nervous system in *Discoglossus pictus* (*Discoglossidae*). Brain Behav Evol. 1997; 50:61–93. [PubMed: 9261554]

Schönberger J, Wang L, Shin JT, Kim SD, Depreux FFS, Zhu H, Zon L, Pizard A, Kim JB, Macrae CA, Mungall AJ, et al. Mutation in the transcriptional coactivator EYA4 causes dilated

cardiomyopathy and sensorineural hearing loss. Nat Genet. 2005; 37:418–422. [PubMed: 15735644]

Stark MR, Sechrist J, Bronner-Fraser M, Marcelle C. Neural tube-ectoderm interactions are required for trigeminal placode formation. Development. 1997; 124:4287–4295. [PubMed: 9334277]

Streit A. Extensive cell movements accompany formation of the otic placode. Dev Biol. 2002; 249:237–254. [PubMed: 12221004]

Streit A. Early development of the cranial sensory nervous system: from a common field to individual placodes. Dev Biol. 2004; 276:1–15. [PubMed: 15531360]

Suzuki T, Takeuchi J, Koshiba-Takeuchi K, Ogura T. *Tbx* genes specify posterior digit identity through Shh and BMP signaling. Dev Cell. 2004; 6:43–53. [PubMed: 14723846]

Takabatake Y, Takabatake T, Takeshima K. Conserved and divergent expression of *T-box* genes *Tbx2-Tbx5* in *Xenopus*. Mech Dev. 2000; 91:433–437. [PubMed: 10704879]

Torres M, Gómez-Pardo E, Gruss P. *Pax2* contributes to inner ear patterning and optic nerve trajectory. Development. 1996; 122:3381–3391. [PubMed: 8951055]

Tucker GC, Delarue M, Zada S, Boucaut JC, Thiery JP. Expression of the HNK-1/NC-1 epitope in early vertebrate neurogenesis. Cell Tissue Res. 1988; 251:457–465. [PubMed: 2449968]

Tümpel S, Sanz-Ezquerro JJ, Isaac A, Eblaghie MC, Dobson J, Tickle C. Regulation of *Tbx3* expression by anteroposterior signalling in vertebrate limb development. Dev Biol. 2002; 250:251–262. [PubMed: 12376101]

van Wijhe JW. Uber die Mesodermsegmente und die Entwicklung der Nerven des Selachierkopfes. Verhandelingen der Koninklijke Akademie van Wetenschappen (Amsterdam). 1882; 22:1–50.

Wayne S, Robertson NG, DeClau F, Chen N, Verhoeven K, Prasad S, Tranebjarg L, Morton CC, Ryan AF, Van Camp G, Smith RJ. Mutations in the transcriptional activator EYA4 cause late-onset deafness at the DFNA10 locus. Hum Mol Genet. 2001; 10:195–200. [PubMed: 11159937]

Yonei-Tamura S, Tamura K, Tsukui T, Izpisúa Belmonte JC. Spatially and temporally-restricted expression of two T-box genes during zebrafish embryogenesis. Mech Dev. 1999; 80:219–221. [PubMed: 10072792]

Europe PMC Funders Author Manuscripts

Europe PMC Funders Author Manuscripts

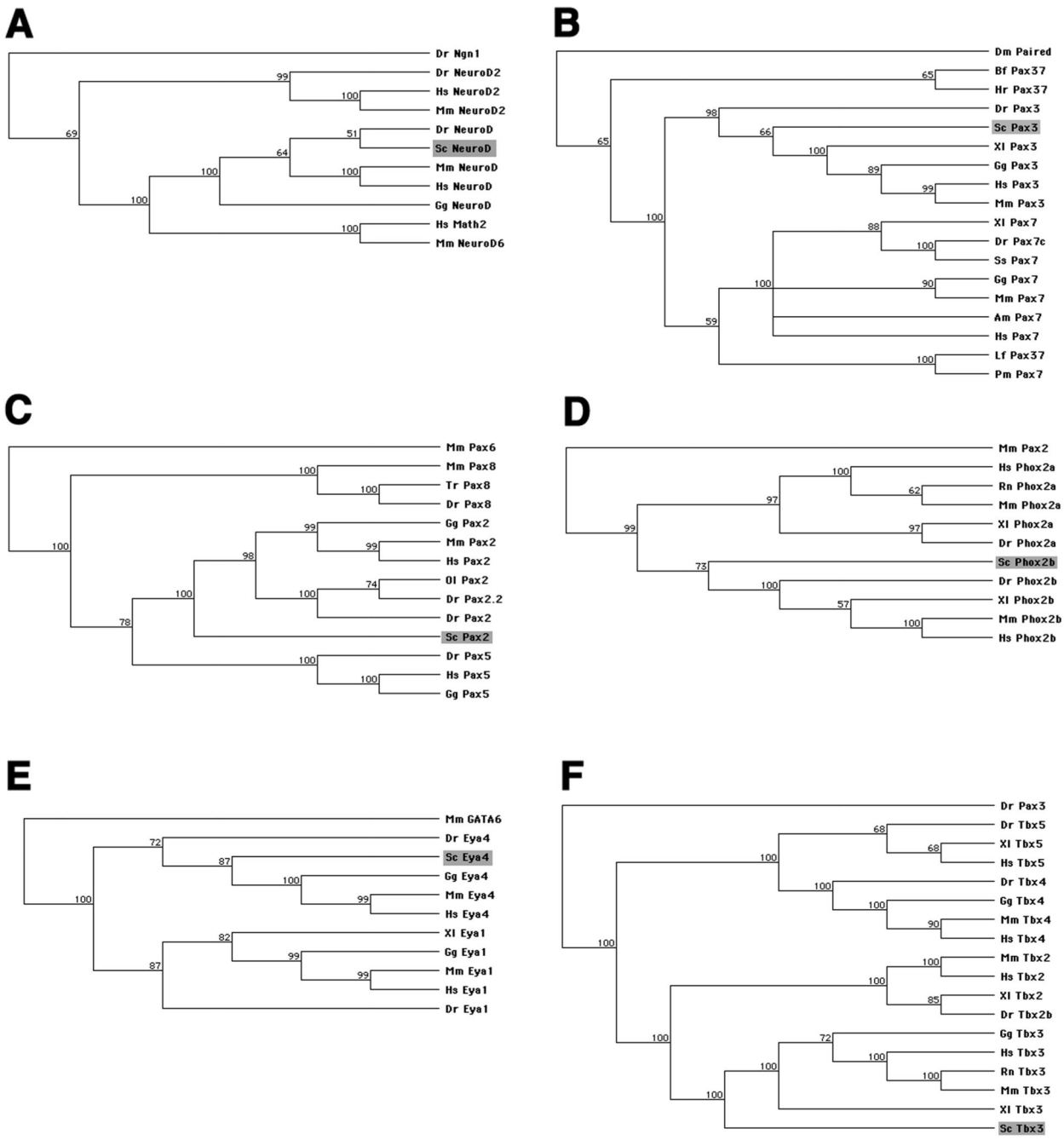

Fig. 1.

Phylogenetic trees, constructed in MacVector using the neighbor-joining method, of predicted protein sequences confirming the identity of cloned fragments of six *S. canicula* transcription factors (shaded box in each tree). Figures adjacent to nodes indicate percentage bootstrap support values. (A) *NeuroD*. (B) *Pax3*. (C) *Pax2*. (D) *Phox2b*. (E) *Eya4*. (F) *Tbx3*. Species abbreviations: Am, *Ambystoma mexicanum*; Bf, *Branchiostoma floridae*; Cf, *Canis familiaris*; Ci, *Ciona intestinalis*; Dm, *Drosophila melanogaster*; Dr, *Danio rerio*; Fr, *Fugu rubripes*; Gg, *Gallus gallus*; Hr, *Halocynthia roretzi*; Hs, *Homo sapiens*; Lf, *Lampetra*

fluviatilis; Mm, *Mus musculus*; Ol, *Oryzias latipes*; Pm, *Petromyzon marinus*; Rn, *Rattus norvegicus*; Sc, *Scyliorhinus canicula*; Ss, *Salmo salar*; Tr, *Takifugu rubripes*; Xl, *Xenopus laevis*.

Europe PMC Funders Author Manuscripts

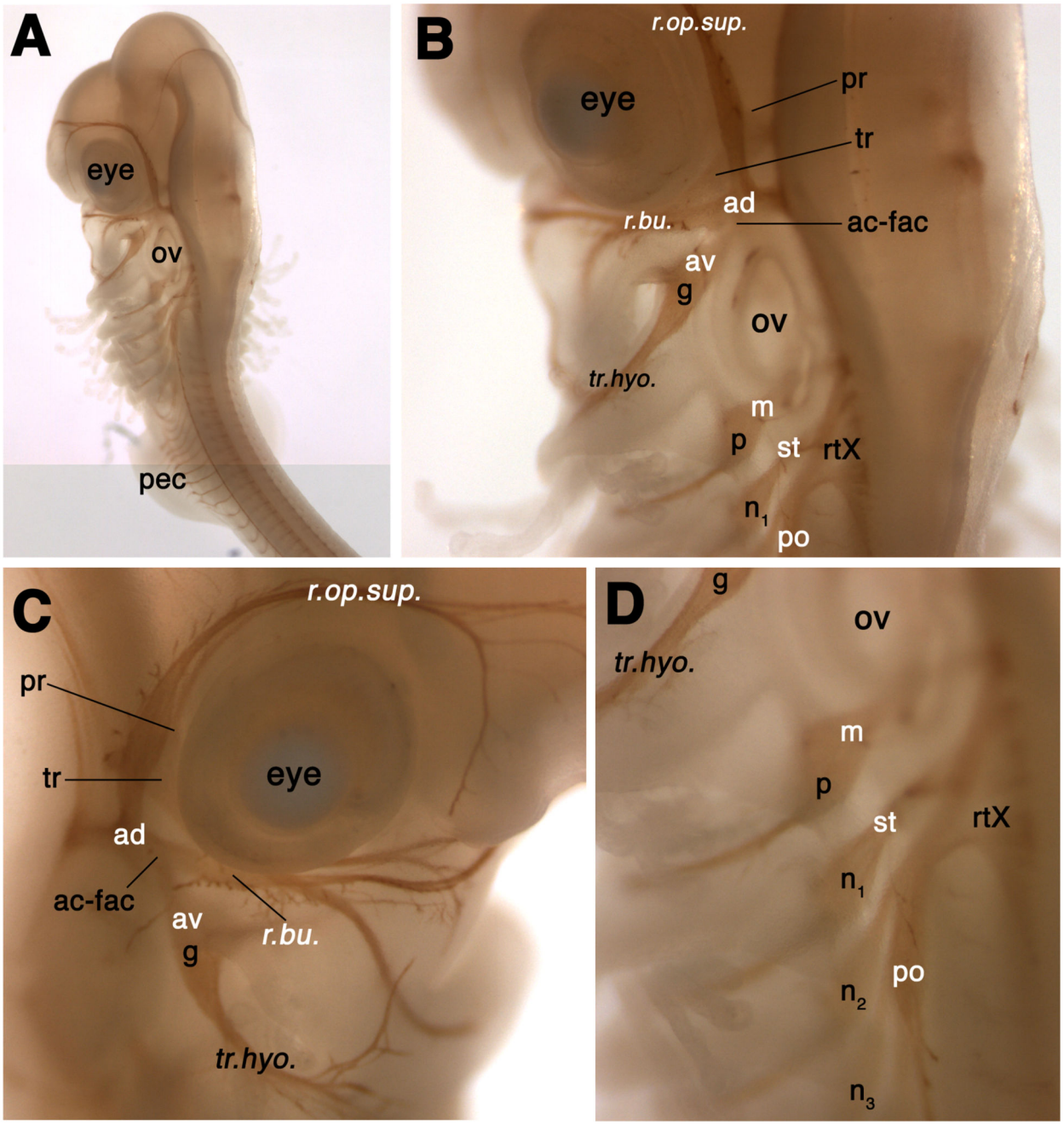

Fig. 2.

Relative positions of the cranial sensory ganglia and associated nerves in a stage 28 (46-51 days) *S. canicula* embryo, immunostained for the neurofilament-associated antigen recognised by the 3A10 antibody. Lateral line and vestibuloacoustic ganglia are labelled in white; nomenclature follows Northcutt (1997). See text for details. Panels B and D are higher-power views of panel A, showing how the profundal (pr) and trigeminal (tr) ganglia are obscured in lateral view by the anterodorsal lateral line ganglion (ad). Panel C is a view of the right side of the embryo's head that shows more clearly the lateral line nerve "twigs"

from the superficial ophthalmic and buccal rami of the anterodorsal lateral line nerve that innervate lateral line organs of the supraorbital and infraorbital lines, respectively. Abbreviations: **ac-fac**, acoustico-facial ganglionic complex; **ad**, anterodorsal lateral line ganglion; **av**, anteroventral lateral line ganglion; **g**, geniculate ganglion; **m**, middle lateral line ganglion; **n**, nodose ganglion; $\mathbf{n_1}$, 1st nodose ganglion; **olf**, olfactory pits; **ov**, otic vesicle; **p**, petrosal ganglion; **pec**, pectoral fin bud; **po**, posterior lateral line ganglion; **pr**, profundal ganglion; ***r.buc.***, buccal ramus of the anterodorsal lateral line nerve; ***r.op.sup.***, superficial ophthalmic ramus of the anterodorsal lateral line nerve; **rtX**, root of the vagus nerve (X); **st**, supratemporal lateral line ganglion; **tr**, trigeminal ganglion; ***tr.hyo***, truncus hyomandibularis.

Europe PMC Funders Author Manuscripts

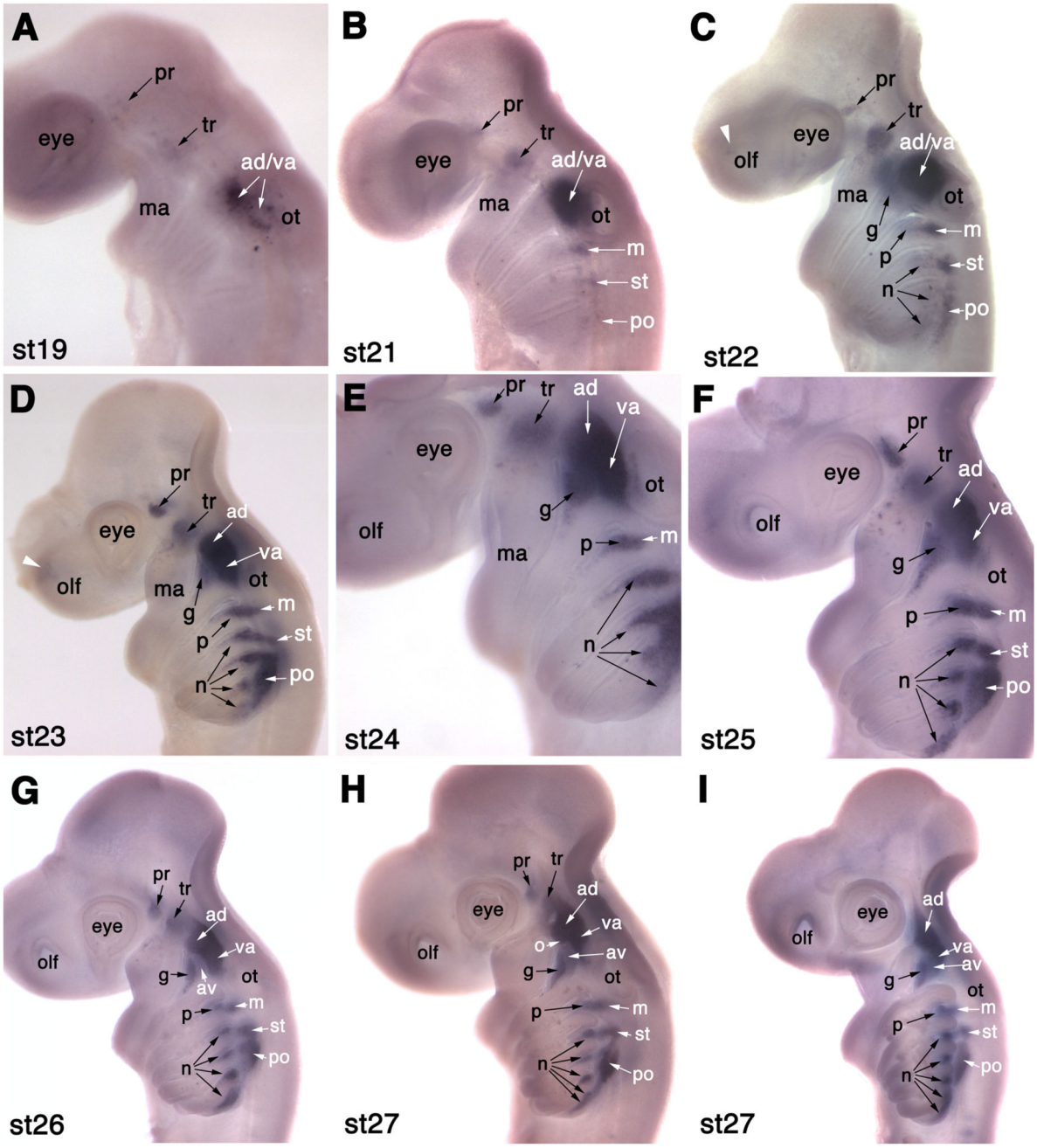

Fig. 3.

NeuroD expression in developing cranial sensory ganglia in *S. canicula*. (A) At stage 19 (22-24 days), *NeuroD* is expressed in a few profundal (pr) neuroblasts behind the eye, a few trigeminal (tr) neuroblasts dorsal to the mandibular arch (ma), and in neuroblasts rostral to the otic placode (ot) that probably include both anterodorsal lateral line (ad) and vestibuloacoustic (va) neuroblasts. (B) At stage 21 (26-27 days), *NeuroD* is also expressed in the forming middle (m) and supratemporal (st) lateral line ganglia, and in a few scattered neuroblasts in the posterior (po) lateral line ganglion. (C) At stage 22 (27-28 days), faint

NeuroD expression is also seen in a few neuroblasts in the region of the future geniculate (g), petrosal (p) and nodose (n) ganglia, and in a faint patch in the olfactory pits (white arrowhead). (D,E) At stages 23 (28-30 days; panel D) and 24 (30-31.5 days; panel E), *NeuroD* expression is seen in a tapering pattern in epibranchial placode-derived neuroblasts (geniculate, g; petrosal, p; nodose, n). The anterodorsal lateral line ganglion (ad) forms the most rostral portion of the ganglionic complex rostral to the otic vesicle. (F) At stage 25 (31-38 days), the profundal (pr) and trigeminal (tr) ganglia seem closer together; the tapering pattern of *NeuroD* expression in the geniculate (g), petrosal (p) and nodose (n) ganglia is still seen though the ganglia are condensing dorsally. (G) At stage 26 (37-42 days), a faint patch of *NeuroD* expression between the geniculate ganglion (g) and the overlying anterodorsal lateral line ganglion (ad) is likely to be the anteroventral lateral line ganglion (av). (H,I) Two different stage 27 (42-46 days) embryos, the younger in panel H. (H) In this stage 27 embryo, the bi-lobed nature of the anterodorsal (ad) lateral line ganglion is more clearly visible, with the rostral (ophthalmic) projection beginning to obscure the trigeminal ganglion (tr). The position of the otic lateral line ganglion (o) is tentatively identified, after Norris and Hughes (1920), at the posterior edge of the buccal (ventral) portion of the anterodorsal lateral line ganglion (ad). (I) In this slightly older stage 27 embryo, both profundal and trigeminal ganglia seem to be obscured in lateral view by the anterodorsal (ad) lateral line ganglion. The geniculate (g), petrosal (p) and nodose (n) ganglia are dense aggregates, apart from the most caudal nodose ganglion that still extends ventrally. The fifth nodose ganglion is now seen as distinct from the fourth. Abbreviations: **ad**, anterodorsal lateral line ganglion; **ad/va**, anterodorsal lateral line/vestibuloacoustic ganglionic complex; **av**, anteroventral lateral line ganglion; **g**, geniculate ganglion; **ma**, mandibular arch; **m**, middle lateral line ganglion; **n**, nodose ganglion; **o**, otic lateral line ganglion; **olf**, olfactory pits; **ot**, otic placode/vesicle; **p**, petrosal ganglion; **pec**, pectoral fin bud; **po**, posterior lateral line ganglion; **pr**, profundal ganglion; **st**, supratemporal lateral line ganglion; **tr**, trigeminal ganglion; **va**, vestibuloacoustic ganglion.

Europe PMC Funders Author Manuscripts

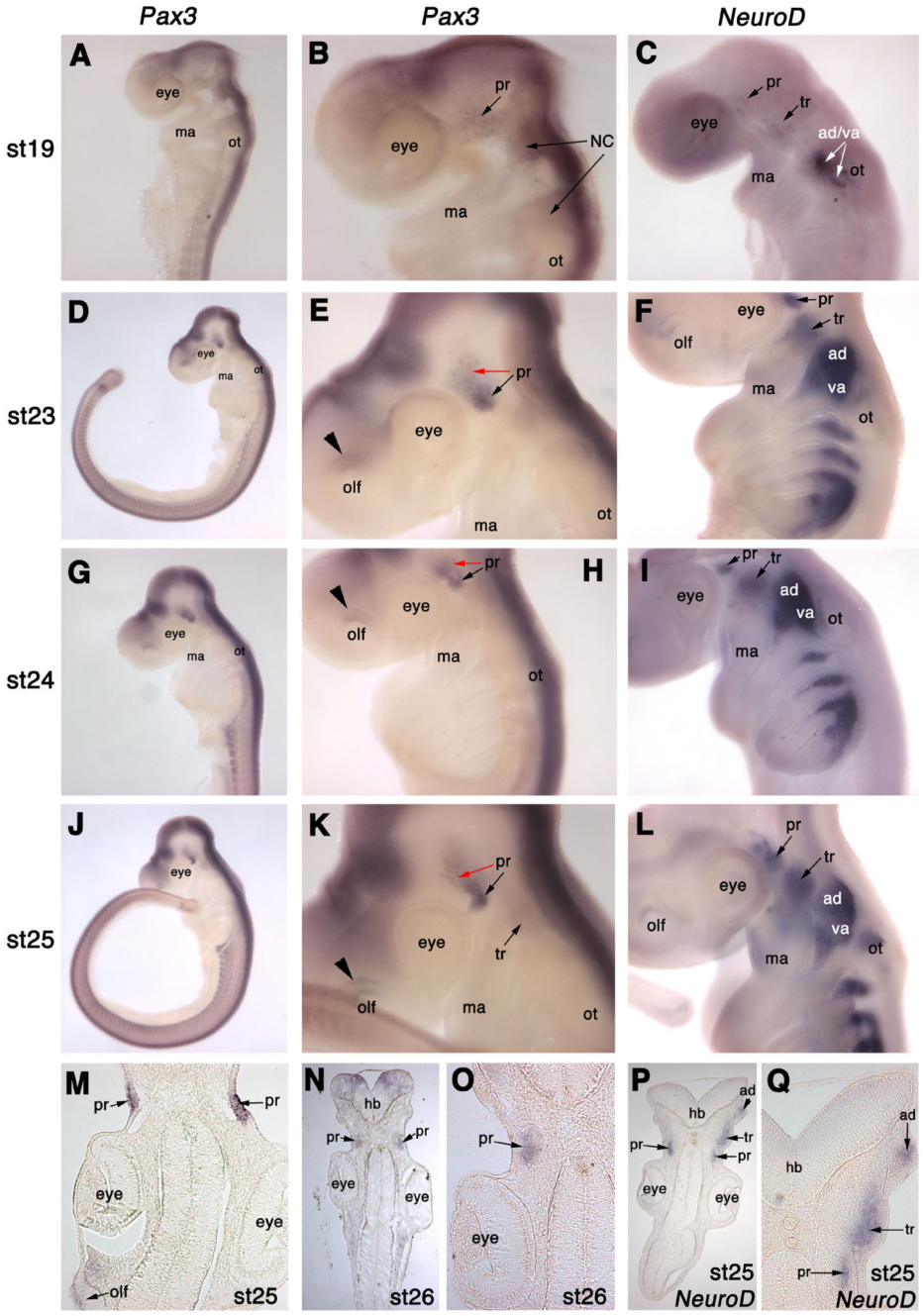

Fig. 4.

Pax3 is expressed in the profundal placode and ganglion in *S. canicula*. (A,B) At stage 19 (22-24 days), *Pax3* is expressed in a salt-and-pepper patch behind the eye, where the profundal placode (pr) forms, and in migrating cranial neural crest cells (NC). (C) For comparison, *NeuroD* expression at stage 19 is seen in a few scattered cells in the profundal placode (pr), the trigeminal placode (tr) dorsal to the mandibular arch (ma), and in the otic vesicle (ot) and forming vestibuloacoustic ganglion. (D,E) At stage 23 (28-30 days), *Pax3* is expressed in a condensed patch, the profundal ganglion (pr, black arrow), as well as in

adjacent ectoderm (profundal placode; red arrow), and in a discrete dorsal region of the olfactory pits (olf; black arrowhead). (F) For comparison, *NeuroD* expression at stage 23 is seen in the profundal (pr) and trigeminal (tr) ganglia, as well as all other placode-derived ganglia (see Fig. 3D for details). (G,H) At stage 24 (30-31.5 days), *Pax3* is expressed in the profundal (pr) placode (red arrow) and ganglion (black arrow), and the dorsal olfactory pits (olf; black arrowhead). The second condensed patch of expression (unlabelled) is the profundal ganglion from the other side of the embryo. (I) For comparison, *NeuroD* expression at stage 24 is seen in the profundal (pr) and trigeminal (tr) ganglia, as well as all other placode-derived ganglia (see Fig. 3E for details). (J,K) At stage 25 (31-38 days), *Pax3* is expressed in the profundal (pr) placode (red arrow) and ganglion (black arrow), as well as very faintly in the trigeminal ganglion (tr; not seen in sections). (L) For comparison, *NeuroD* expression at stage 25 is seen in all placode-derived ganglia (see Fig. 3F for details). (M) Section through a stage 25 embryo after wholemount *in situ* hybridisation for *Pax3*, showing *Pax3* expression in the profundal placodes (pr) and very faintly in the olfactory pits (olf). (N,O) Section through a stage 26 (37-42 days) embryo after wholemount *in situ* hybridisation, showing *Pax3* expression in the profundal ganglia (pr). (P,Q) Section through a stage 25 embryo after wholemount *in situ* hybridisation for *NeuroD*, showing *NeuroD* expression in the profundal (pr), trigeminal (tr) and anterodorsal lateral line (ad) ganglia. Abbreviations: **ad**, anterodorsal lateral line ganglion; **ad/va**, anterodorsal lateral line/ vestibuloacoustic ganglionic complex; **hb**, hindbrain; **ma**, mandibular arch; **NC**, neural crest; **olf**, olfactory pits; **ot**, otic vesicle; **pr**, profundal ganglion; **st**, stage; **tr**, trigeminal ganglion; **va**, vestibuloacoustic ganglion.

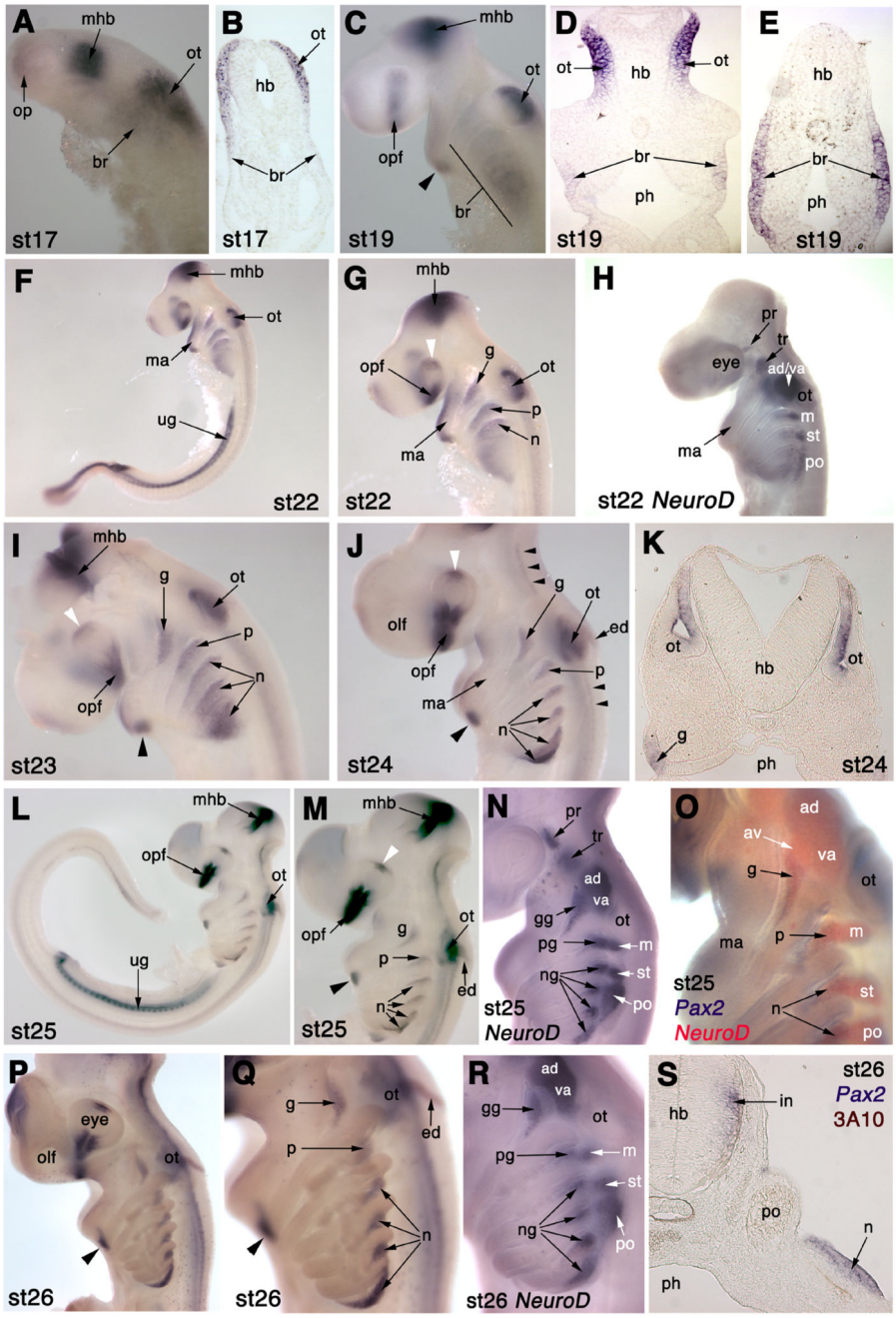

Fig. 5.

Pax2 is expressed in both otic and epibranchial placodes in *S. canicula*. (A,B) At stage 17 (16-20 days), *Pax2* is expressed strongly in the thickened ectoderm of the developing otic placode (ot) and, more faintly, in ectoderm in the branchial region (br). It is also expressed in the optic vesicles (op) and in the midbrain-hindbrain border region (mhb). (C-E) At stage 19 (22-24 days), *Pax2* is expressed in the dorsomedial region of the invaginating otic placodes (ot) and more faintly in branchial ectoderm (br). It is also expressed in the optic fissure (opf), the midbrain-hindbrain border (mhb), and in a ventral patch (arrowhead) in the

mandibular arch (ma). (F,G) At stage 22 (27-28 days), *Pax2* is expressed in the dorsomedial otic vesicle (ot) and in broad dorsal stripes caudal to the forming pharyngeal clefts/pouches, the forming epibranchial placodes (g, geniculate; p, petrosal; n_1, first nodose placode). It is also expressed in the optic fissure (opf), the dorsal optic cup (white arrowhead), the midbrain-hindbrain border (mhb) and the urogenital tract (ug). (H) For comparison, *NeuroD* at stage 22 is only just beginning to be expressed in the most dorsal regions of the pharyngeal arches where the epibranchial placodes are forming, ventral to the acousticofacial ganglionic complex (ac-fac) and the post-otic lateral line ganglia (see Fig. 3C for details). (I) At stage 23 (28-30 days), *Pax2* expression is more clearly seen in the forming epibranchial placodes (g, geniculate; p, petrosal; n, nodose), as well as in the dorsomedial otic vesicle (ot), the developing thyroid gland (black arrowhead) at the base of the mandibular arch, the optic fissure (opf), the dorsal optic cup (white arrowhead), and the midbrain-hindbrain border (mhb; slightly damaged in this embryo). (J) At stage 24 (30-31.5 days), *Pax2* is expressed much as described in panel (I), and also now in the developing endolymphatic duct (ed) and in bilateral stripes of interneurons in the hindbrain and spinal cord (small black arrowheads). White arrowhead: dorsal optic cup; black arrowhead: thyroid gland. (K) A section through the otic vesicle (ot) and geniculate placode (g) at stage 24 shows more clearly the restriction of *Pax2* expression to the dorsomedial region of the otic vesicle. (L,M) At stage 25 (31-38 days), *Pax2* expression continues in all domains previously described, with further resolution of the epibranchial placodes (g, geniculate; p, petrosal; n, nodose). White arrowhead: dorsal optic cup; black arrowhead: thyroid gland. (N,O) For comparison, *NeuroD* at stage 25 (*NeuroD* alone in panel N; double *in situ* hybridsation for *Pax2* [blue] and *NeuroD* [red] in panel O) confirms restriction of *Pax2* expression to the epibranchial placodes, with no overlap in expression in the more dorsal lateral line ganglia (av, anteroventral; ad, anterodorsal; m, middle; st, supratemporal; po, posterior). (P,Q) At stage 26 (37-42 days), *Pax2* expression in the epibranchial placodes has resolved to the most dorsal region of the pharyngeal arches except for the most caudal nodose placode (n), where *Pax*2 expression extends much further ventrally. Scattered $Pax2^+$ cells throughout the embryo may be macrophages. Black arrowhead: thyroid gland. (R) For comparison, *NeuroD* expression at stage 26 also shows neurogenesis occurring more ventrally in the most caudal nodose placode, though it does not extend as far ventrally as *Pax2* expression. (S) Section of a stage 26 *Pax2*-hybridised embryo through the posterior lateral line ganglion region (po), immunostained for neurofilament (3A10 antibody; brown) shows that *Pax2* expression in the epibranchial placodes (represented here by one of the nodose placodes, n) is confined to the thickened placodal ectoderm. *Pax2* is also expressed by hindbrain interneurons (in). Abbreviations: **ac-fac**, acoustico-facial ganglionic complex; **ad**, anterodorsal lateral line ganglion; **ad/va**, anterodorsal lateral line/vestibuloacoustic ganglionic complex; **av**, anteroventral lateral line ganglion; **br**, branchial ectoderm; **ed**, endolymphatic duct; **g**, geniculate placode; **gg**, geniculate ganglion; **hb**, hindbrain; **in**, interneurons; **ma**, mandibular arch; **m**, middle lateral line ganglion; **mhb**, midbrain-hindbrain border region; **n**, nodose placode; **ng**, nodose ganglion; **olf**, olfactory pits; **op**, optic vesicles; **opf**, optic fissure; **ot**, otic placode/vesicle; **p**, petrosal placode; **pg**, petrosal ganglion; **ph**, pharynx; **po**, posterior lateral line ganglion; **pr**, profundal ganglion; **st**, supratemporal lateral line ganglion; **tr**, trigeminal ganglion; **ug**, urogenital tract; **va**, vestibuloacoustic ganglion.

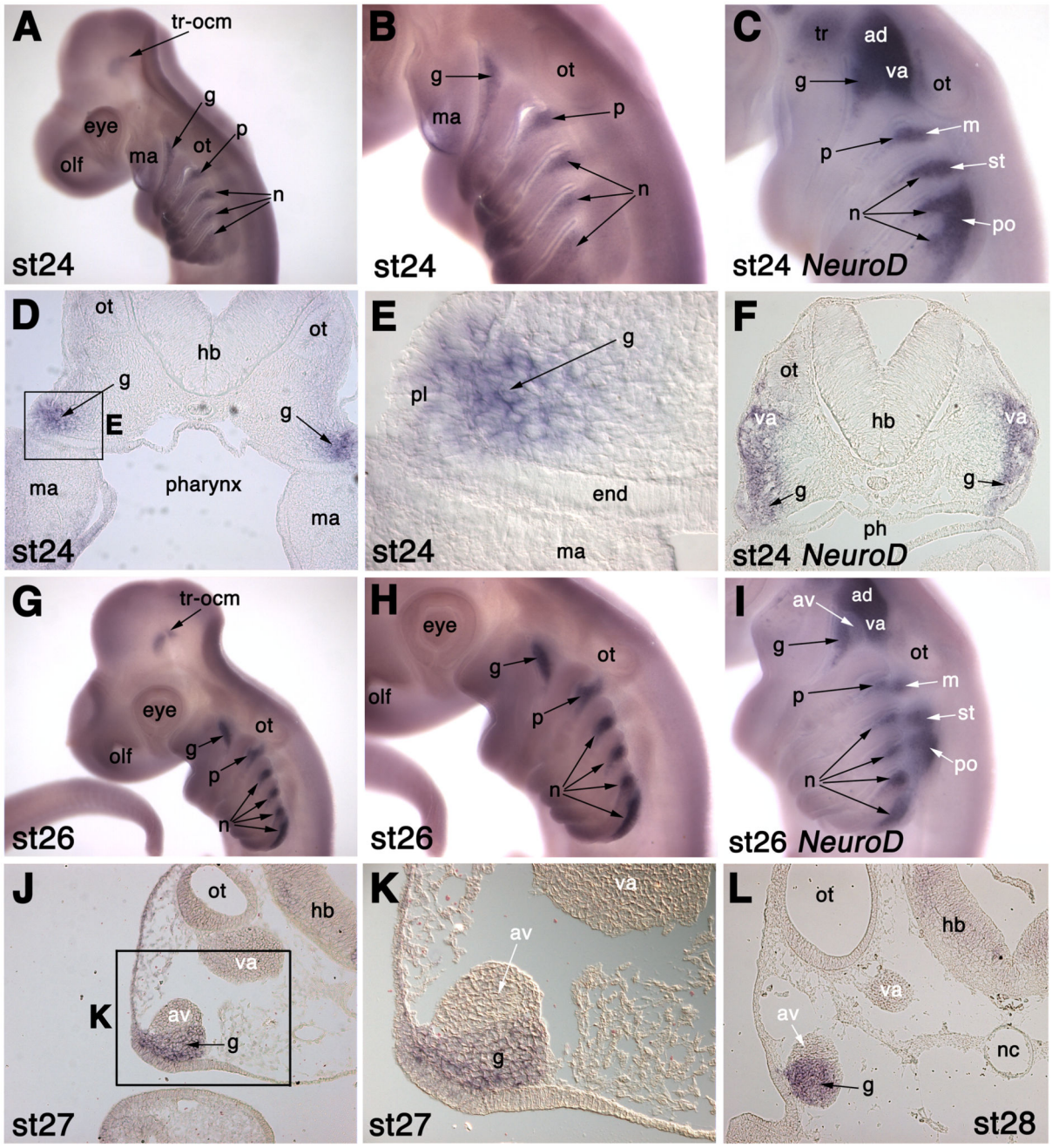

Fig. 6.

Phox2b is expressed in epibranchial placode-derived neurons in *S. canicula*. (A,B) At stage 24 (30-31.5 days), *Phox2b* is specifically expressed in the developing epibranchial placode-derived ganglia (g, geniculate; p, petrosal; n, nodose), and in the trochlear and oculomotor nuclei (tr-ocm). (C) *NeuroD* expression at stage 24 for comparison with panel B. (D,E) Section at the otic vesicle (ot) level of a stage 24 embryo after *in situ* hybridisation for *Phox2b* (panel E is a higher-power view of boxed area in panel D), showing *Phox2b* expression both in geniculate placode-derived neuroblasts (g) and also in some cells in the

Europe PMC Funders Author Manuscripts

Europe PMC Funders Author Manuscripts

geniculate placode (pl) itself. (F) Section of a stage 24 embryo at the same level after *in situ* hybridisation for *NeuroD*, for comparison with panels D and E. (G,H) At stage 26 (37-42 days), *Phox2b* is specifically expressed in the epibranchial placode-derived ganglia (g, geniculate; p, petrosal; n, nodose) and in the trochlear and oculomotor nuclei (tr-ocm). (I) *NeuroD* expression at stage 26 for comparison with panel H. (J,K) Section at the otic vesicle (ot) level of a stage 27 embryo after *in situ* hybridisation for *Phox2b* (panel K is a higher-power view of boxed area in panel J). *Phox2b* is specifically expressed in the geniculate ganglion (g), but not in the anteroventral lateral line ganglion (av) with which it is in close contact, or in the vestibuloacoustic ganglion (va). (L) Section of a stage 28 embryo after *in situ* hybridisation for *Phox2b*, at the same level as in panels J,K, confirming *Phox2b* expression specifically in the geniculate ganglion (g) and not in either the anteroventral lateral line ganglion (av) or vestibuloacoustic ganglion (va). Abbreviations: **ac-fac**, acoustico-facial ganglionic complex; **ad**, anterodorsal lateral line ganglion; **av**, anteroventral lateral line ganglion; **end**, pharyngeal endoderm; **g**, geniculate ganglion; **hb**, hindbrain; **ma**, mandibular arch; **m**, middle lateral line ganglion; **n**, nodose ganglion; **nc**, notochord; **olf**, olfactory pits; **ot**, otic vesicle; **p**, petrosal ganglion; **ph**, pharynx; **pl**, placode ectoderm; **po**, posterior lateral line ganglion; **st**, supratemporal lateral line ganglion; **tr**, trigeminal ganglion; **tr-ocm**, trochlear and oculomotor nuclei; **va**, vestibuloacoustic ganglion.

Europe PMC Funders Author Manuscripts

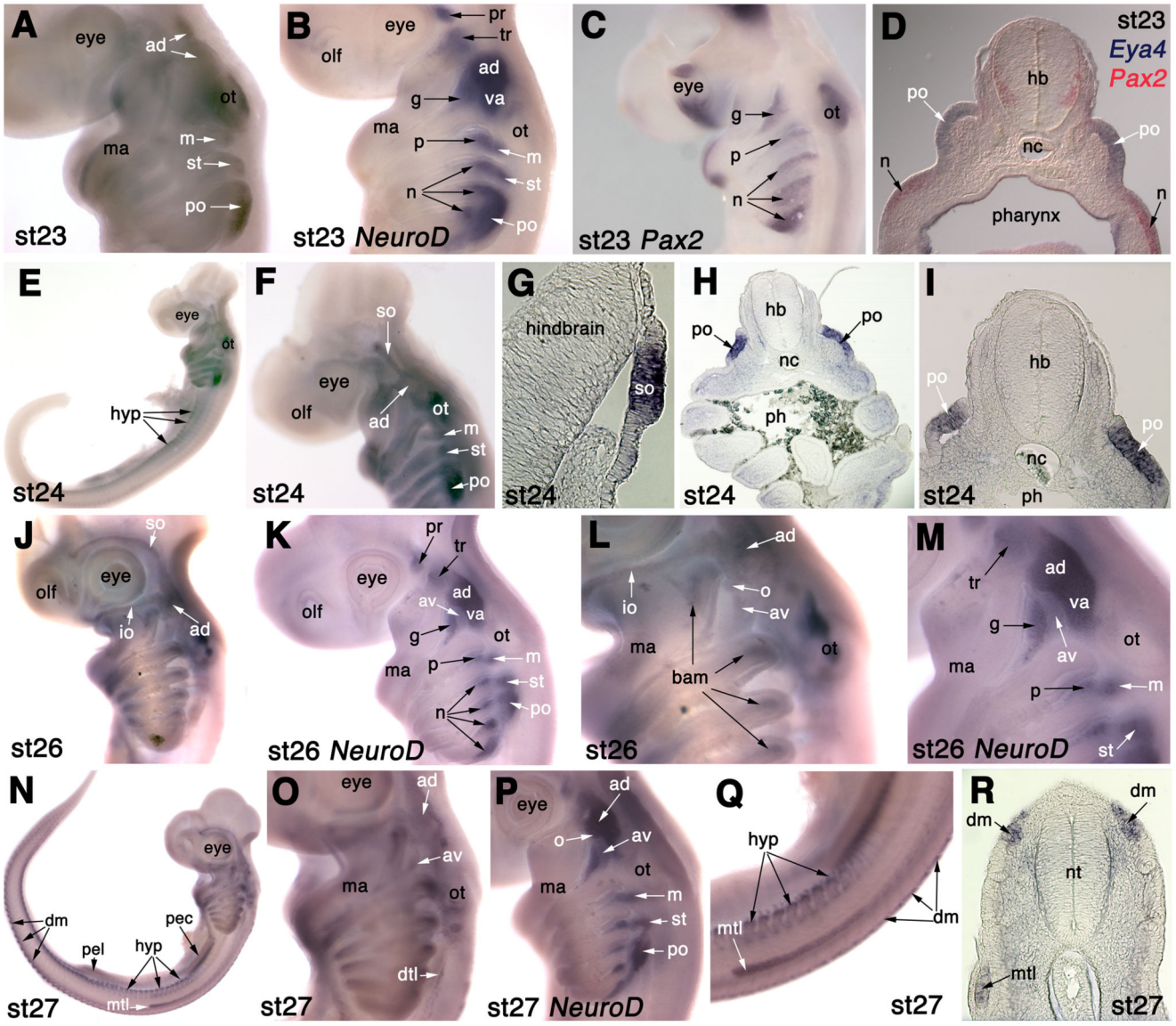

Fig. 7.

Eya4 is expressed in lateral line placodes in *S. canicula*. (A) At stage 23 (28-30 days), *Eya4* is expressed in the anterodorsal lateral line placode (ad), including a rostral extension (upper arrow) likely to be the start of formation of the supraorbital sensory ridge, as well as in the middle (m), supratemporal (st) and posterior (po) lateral line placodes, and in the otic vesicle (ot). (B) *NeuroD* expression at stage 23 for comparison with panel A. (C) *Pax2* expression at stage 23 for comparison with panel A. (D) A section through an embryo after double *in situ* hybridisation for *Eya4* (blue) and *Pax2* (red) at the level of the posterior lateral line placode (po) confirms *Eya4* expression in lateral line placode ectoderm only, dorsal to a nodose placode (n). (E,F) At stage 24 (30-31.5 days), *Eya4* is expressed in the anterodorsal lateral line placode (ad) and in the supraorbital ridge (so) extending from it, as well as in the middle (m), supratemporal (st) and posterior (po) lateral line placodes, and in the otic vesicle (ot). It is also expressed in hypaxial muscle primordia (hyp) in the trunk. (G-I) Sections through the

stage 24 embryo shown in panels E and F. (G) Section through the *Eya4*$^{+}$ supraorbital sensory ridge (so) projecting from the anterodorsal lateral line placode. (H,I) Sections through the posterior lateral line placode (po), confirming restriction of *Eya4* expression to lateral line placode ectoderm, with much fainter expression in branchial arch mesenchyme. (J,L) At stage 26 (37-42 days), *Eya4* is expressed in the supraorbital (so) and infraorbital (io) ridges extending from the anterodorsal lateral line placode (ad), as well as in the otic vesicle (ot) and in stripes in the branchial arches that are most likely branchial arch muscle primordia (bam). A circular patch of *Eya4* expression projecting from the caudoventral border of the *Eya4*$^{+}$ anterodorsal lateral line placode (ad) may represent the otic lateral line placode (o). Further ventrally, another faint patch of *Eya4* expression is likely to represent the anteroventral lateral line placode (av). (K,M) *NeuroD* expression at stage 26 for comparison with panels J and L, showing the respective positions of the geniculate (g) and anteroventral lateral line (av) ganglia. (N) At stage 27 (42-46 days), *Eya4* is expressed in the dorsal dermomyotome (dm) and hypaxial muscle primordia (hyp). The migrating *Eya4*$^{+}$ main trunk line (mtl) primordium has reached a point midway between the pectoral (pec) and pelvic (pel) fin buds. (O) Higher-power view of the head of the embryo in panel N, showing *Eya4* expression in the anterodorsal (ad) and anteroventral (av) lateral line placodes, and the beginning of the dorsal trunk line (dtl). Expression in the middle and supratemporal lateral line placodes is no longer seen (compare with panel F), while the main trunk line (mtl) primordium has migrated onto the trunk (see panels N,Q). (P) *NeuroD* expression at stage 27 for comparison with panel O. The position of the otic lateral line ganglion (o) is tentatively identified, after Norris and Hughes (1920), at the posterior edge of the buccal (ventral) portion of the anterodorsal lateral line ganglion (ad; compare with position of the otic lateral line placode in panel L). (Q) Higher-power view of the trunk of the embryo in panel N, showing *Eya4* expression in the migrating main trunk line (mtl) primordium, hypaxial muscle primordia (hyp) and the dorsal tip of the dermomyotome (dm). (R) Section through the trunk of a stage 27 embryo, showing *Eya4* expression in the migrating main trunk line (mtl) primordium, and in the dorsal tip of the dermomyotome (dm). Abbreviations: **ad**, anterodorsal lateral line placode/ganglion; **av**, anteroventral lateral line placode/ganglion; **dm**, dorsal dermomyotome; **dtl**, dorsal trunk line; **g**, geniculate placode/ganglion; **hb**, hindbrain; **hyp**, hypaxial muscle primordia; **io**, infraorbital sensory ridge; **m**, middle lateral line placode/ganglion; **ma**, mandibular arch; **mtl**, main trunk line primordium; **n**, nodose placode/ganglion; **nc**, notochord; **o**, otic lateral line placode/ganglion; **olf**, olfactory pits; **ot**, otic vesicle; **p**, petrosal ganglion; **pec**, pectoral fin bud; **pel**, pelvic fin bud; **ph**, pharynx; **pl**, placode ectoderm; **po**, posterior lateral line placode/ganglion; **so**, supraorbital sensory ridge; **st**, supratemporal lateral line placode/ganglion; **tr**, trigeminal ganglion; **va**, vestibuloacoustic ganglion.

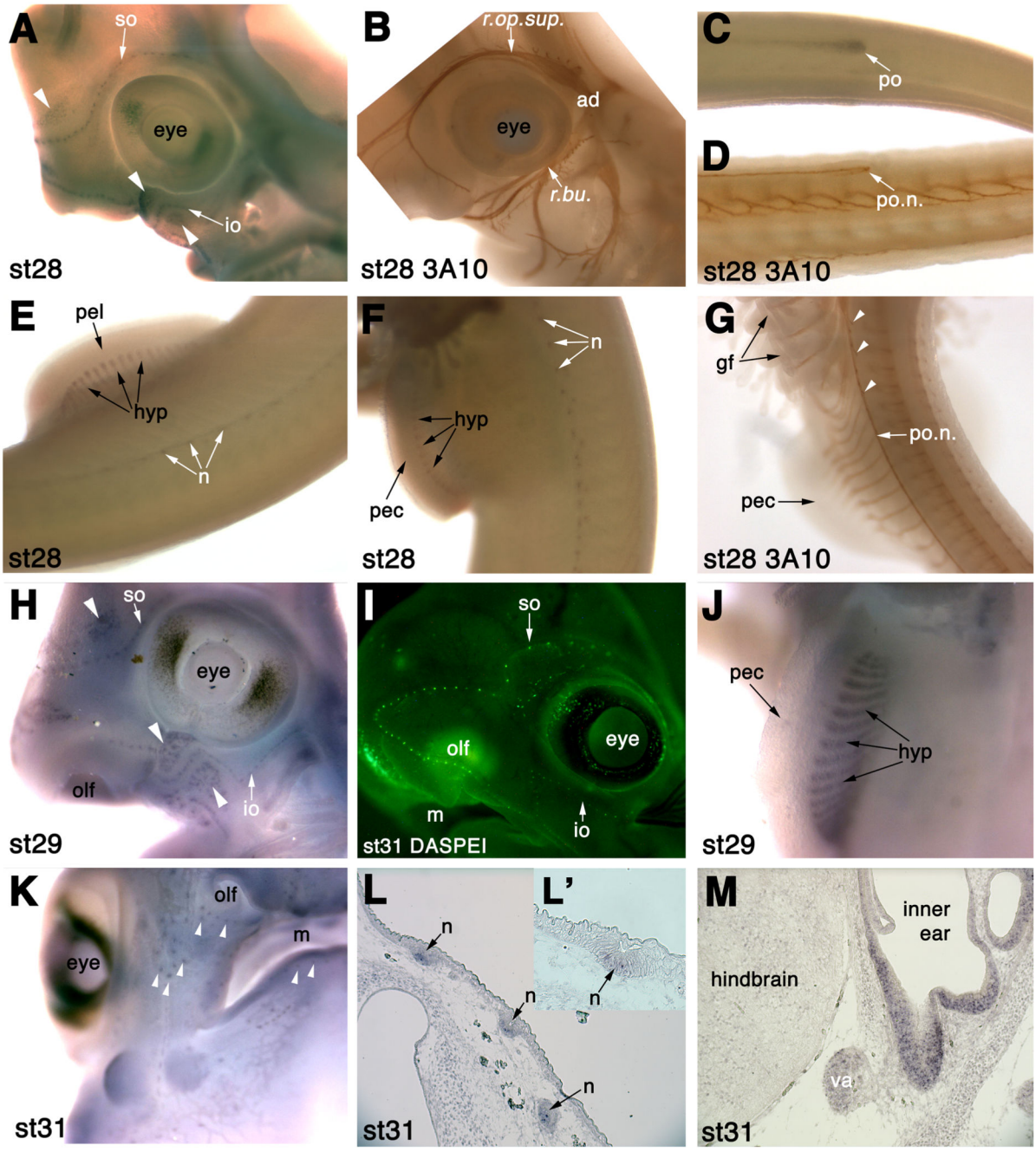

Fig. 8.

Eya4 is expressed in differentiating lateral line sense neuromasts and ampullary organs in *S. canicula*. (A) At stage 28 (46-51 days), *Eya4* is expressed in individual lateral line neuromasts in the supraorbital (so) and infraorbital (io) lateral lines, and in developing ampullary organ fields dorsal and ventral to these lines (white arrowheads). (B) Head of a 3A10 (neurofilament)-immunostained stage 28 embryo for comparison with panel A, showing "twigs" from the superficial ophthalmic ramus (sup.op.r.) and buccal ramus (bucc.r.) of the anterodorsal lateral line nerve, that innervate neuromasts of the supraorbital

Europe PMC Funders Author Manuscripts

and infraorbital lateral lines, respectively. (C) *Eya4* expression in the migrating posterior lateral line primordium (po) on the trunk at stage 28. Dorsal is to the top of the panel. (D) 3A10 immunostaining at stage 28 for comparison with panel C, showing the posterior lateral line nerve (po.n.) extending into the migrating posterior lateral line primordium. Dorsal is to the top of the panel. (E) *Eya4* expression at stage 28 in trunk lateral line neuromasts (n) and in hypaxial muscle primordia (hyp) in the pelvic fin (pel). (F) *Eya4* expression at stage 28 in trunk lateral line neuromasts (n) and in hypaxial muscle primordia (hyp) in the pectoral fin (pec). (G) 3A10 immunostaining at stage 28 for comparison with panels E and F, showing "twigs" from the posterior lateral line nerve (po.n.) that innervate trunk lateral line neuromasts. (H) At stage 29 (49-53 days), *Eya4* is expressed in lateral line neuromasts of the supraorbital (so) and infraorbital (io) lateral lines, and in individual ampullary organs in the ampullary fields dorsal and ventral to these lines (white arrowheads). (I) DASPEI-stained embryo at stage 31 (60-80 days) for comparison with panel H, showing position of neuromasts in the supraorbital (so) and infraorbital (io) lateral lines. (J) At stage 29, *Eya4* is still expressed in hypaxial muscle primordia (hyp) in the pectoral fin bud (pec). (K) At stage 31 (60-80 days), *Eya4* is still expressed in lateral line neuromasts and ampullary organs (white arrowheads). (L,L') *In situ* hybridisation on sections of a stage 31 embryo (higher power in panel L'), showing *Eya4* expression in a centrally located subset of cells in lateral line neuromasts (n). (M) *In situ* hybridisation on a section of a stage 31 embryo, showing *Eya4* expression in the sensory epithelium of the inner ear, as well as more faintly in the vestibuloacoustic ganglion (va). Abbreviations: **ad**, anterodorsal lateral line ganglion; **gf**, gill filament; **hyp**, hypaxial muscle primordia; **io**, infraorbital lateral line; **m**, mouth; **n**, neuromast; **olf**, olfactory pits; **pec**, pectoral fin bud; **pel**, pelvic fin bud; **po**, posterior lateral line primordium; **po.n.**, posterior lateral line nerve; ***r.buc.***, buccal ramus of the anterodorsal lateral line nerve; ***r.op.sup.***, superficial ophthalmic ramus of the anterodorsal lateral line nerve; **so**, supraorbital lateral line; **va**, vestibuloacoustic ganglion.

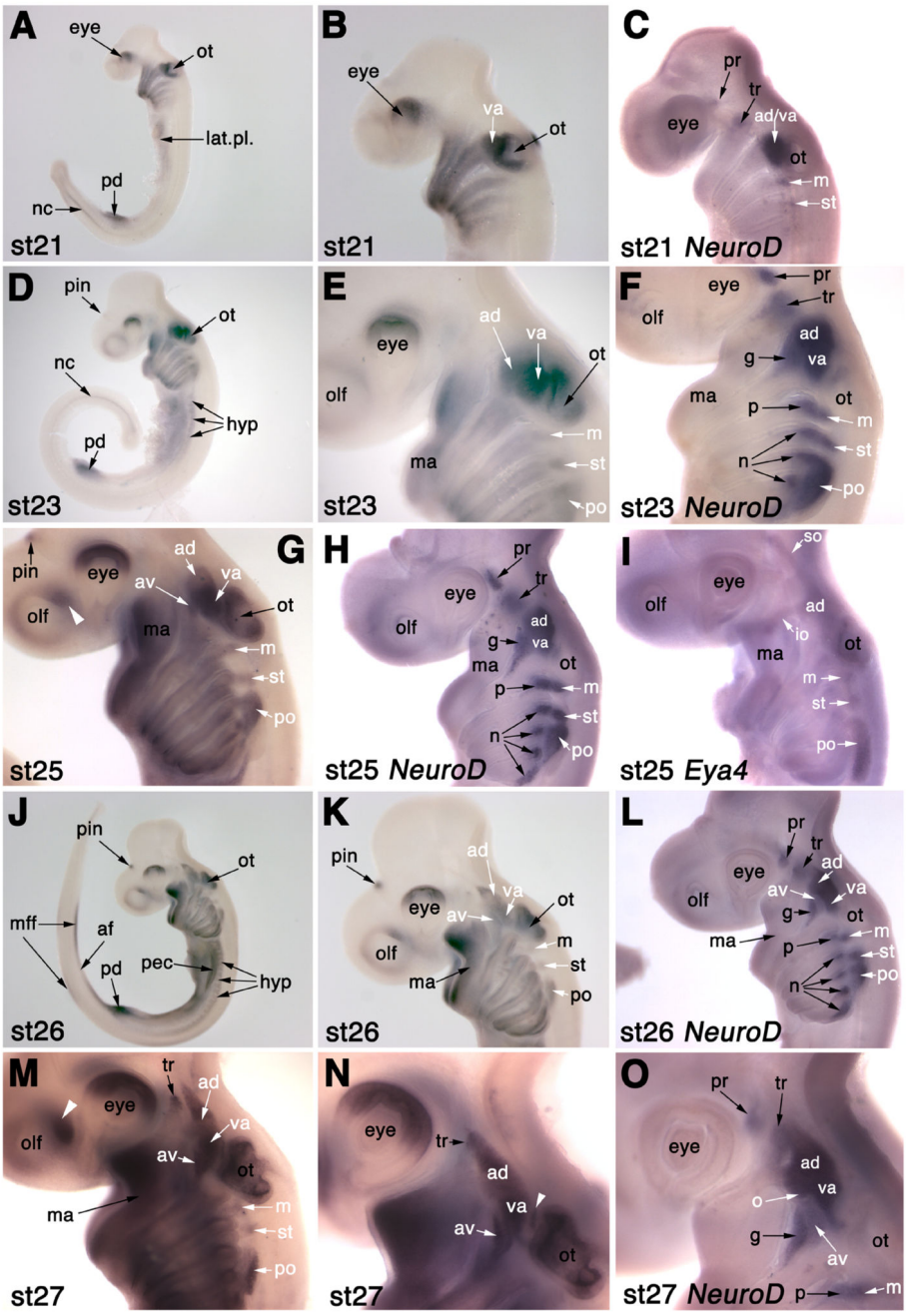

Fig. 9.

Tbx3 is expressed in lateral line and vestibuloacoustic ganglia in *S. canicula*. (A,B) At stage 21 (26-27 days), *Tbx3* is expressed in the otic placode (ot), vestibuloacoustic ganglion (va), dorsal retina, branchial arches, anterior lateral plate mesoderm (lat.pl.), proctodeum (pd) and posterior notochord (nc). (C) *NeuroD* expression at stage 21 for comparison with panel B. (D,E) At stage 23 (28-30 days), *Tbx3* is additionally expressed in the anterodorsal (ad), middle (m), supratemporal (st) and posterior (po) lateral line ganglia, as well as hypaxial muscle primordia (hyp) and very faintly in the pineal gland (pin). (F) *NeuroD* expression at

stage 23 for comparison with panel E. (G) At stage 25 (31-38 days), *Tbx3* expression is maintained in lateral line and vestibuloacoustic ganglia, in the pineal gland (pin), dorsal retina, a patch dorsal to the olfactory pits (white arrowhead) and branchial arches (most strongly in the mandibular arch, ma). (H) *NeuroD* expression at stage 25 for comparison with panel G. (I) Expression of the lateral line placode marker *Eya4* at stage 25, for comparison with panel G. (J,K) At stage 26 (37-42 days), *Tbx3* expression is also seen in the pectoral fin bud (pec) and the median fin-fold (mff) except in the position of the future anal fin (af). (L) *NeuroD* expression at stage 26 for comparison with panel K. (M,N) Left side (M) and right side (N, flipped horizontally for easier comparison) of a stage 27 embryo, showing *Tbx3* expression in the trigeminal ganglion (tr), anterodorsal (ad) and anteroventral (av) lateral line ganglia, the three post-otic lateral line ganglia (middle, supratemporal, posterior), and at least part of the vestibuloacoustic ganglion (va): expression seems to have been lost in the region abutting the rostral edge of the otic vesicle (ot; compare with panel G), apart from a thin stripe (arrowhead). (O) *NeuroD* expression at stage 27 for comparison with panels M and N. Note the apparent loss of *NeuroD* expression from the region abutting the rostral edge of the otic vesicle (compare with panel H). Abbreviations: **ad**, anterodorsal lateral line placode/ganglion; **ad/va**, anterodorsal lateral line/vestibuloacoustic ganglionic complex; **af**, anal fin; **av**, anteroventral lateral line ganglion; **g**, geniculate ganglion; **hyp**, hypaxial muscle primordia; **io**, infraorbital sensory ridge; **m**, middle lateral line placode/ganglion; **ma**, mandibular arch; **mff**, median fin-fold; **n**, nodose ganglion; **o**, otic lateral line ganglion; **olf**, olfactory pits; **ot**, otic placode/vesicle; **p**, petrosal ganglion; **pd**, proctodeum; **pec**, pectoral fin bud; **pin**, pineal gland; **po**, posterior lateral line placode/ganglion; **pr**, profundal ganglion; **po.pr.**, posterior lateral line primordium; **so**, supraorbital sensory ridge; **st**, supratemporal lateral line placode/ganglion; **tr**, trigeminal ganglion; **va**, vestibuloacoustic ganglion.

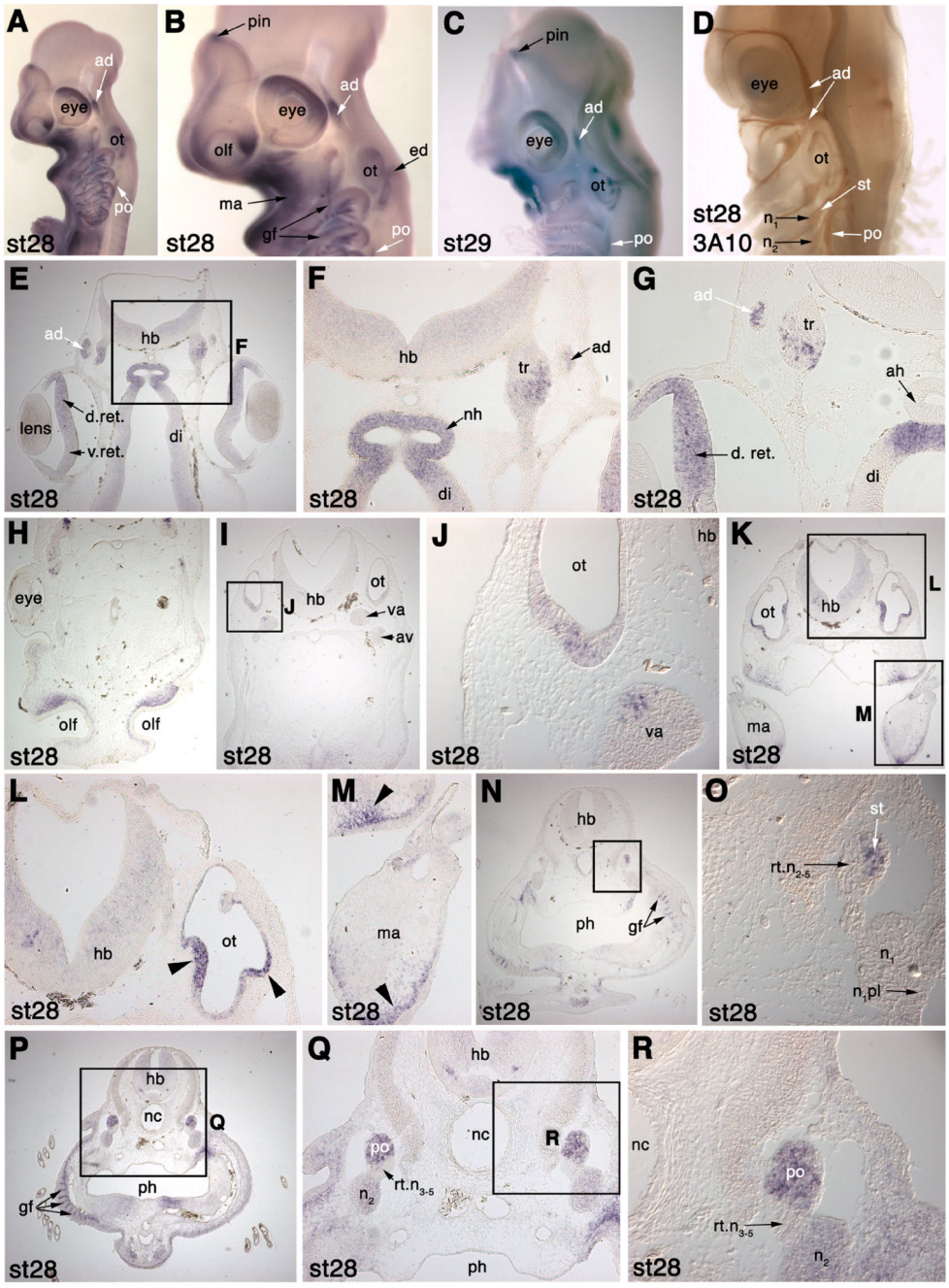

Fig. 10.

Tbx3 expression at stages 28-29 (46-53 days) in *S. canicula*. (A,B) At stage 28 (46-51 days), *Tbx3* expression is seen in whole-mount in the rostralmost projection of the anterodorsal lateral line ganglion (ad) and in the posterior lateral line ganglion (po), in the otic vesicle (ot) and endolymphatic duct (ed), dorsal retina, pineal gland (pin), branchial arches (most strongly in the mandibular arch, ma) and gill filaments (gf). (C) At stage 29 (49-53 days), *Tbx3* is expressed similarly, with expression in the otic vesicle confined to several specific regions (possibly sensory patches). (D) 3A10 (neurofilament)-immunostained embryo at

stage 28 for comparison with panel C and for orientation relative to panels N-R. (E-R) *In situ* hybridisation for *Tbx3* on transverse sections of a stage 28 embryo. (E-G) Transverse sections at the level of the eye, showing *Tbx3* expression in the anterodorsal lateral line ganglion (ad), a subset of trigeminal ganglion (tr) cells, the dorsal retina (d.ret.), and the neurohypophysis (nh) and surrounding neural ectoderm in the floor of the diencephalon (di). The adenohypophysis (ah, in panel G) is *Tbx3*-negative. (H) Transverse section at the level of the eye and olfactory pits (olf), showing *Tbx3* expression in mesenchyme at the dorsal edge of the olfactory pits. (I,J) Transverse section at the level of the otic vesicle (ot), showing *Tbx3* expression in a subset of vestibuloacoustic ganglion (va) cells and a restricted patch of otic epithelium. (K-M) Transverse section at the level of the otic vesicle (ot), showing *Tbx3* expression in restricted regions of otic epithelium (possibly sensory patches; black arrowheads in L) and in mesenchyme at the edge of the mandibular arch (ma; black arrowheads in M). (N,O) Transverse section at the level of the first nodose ganglion (n_1) and placode ($n_1$pl; compare with panel D), showing *Tbx3* expression specifically in the supratemporal lateral line ganglion (st), and not in either the nodose ganglion or the root of the more caudal nodose ganglia (rt.$n_{2\text{-}5}$; identification based on (Landacre, 1916). (P-R) Transverse section at the level of the second nodose ganglion (n_2; compare with panel D), showing *Tbx3* expression specifically in the posterior lateral line ganglion (po), and not in either the nodose ganglion or the root of the more caudal nodose ganglia (rt.$n_{3\text{-}5}$; identification based on (Landacre, 1916). Abbreviations: **ad**, anterodorsal lateral line ganglion; **ah**, adenohypophysis; **d.ret.**, dorsal retina; **di**, diencephalon; **ed**, endolymphatic duct; **gf**, gill filaments; **hb**, hindbrain; **ma**, mandibular arch; **n**, nodose ganglion; **n_1**, first nodose ganglion; **$n_1$pl**, first nodose placode; **n_2**, second nodose ganglion; **nc**, notochord; **nh**, neurohypophysis; **olf**, olfactory pits; **ot**, otic vesicle; **ph**, pharynx; **pin**, pineal gland; **po**, posterior lateral line ganglion; **rt.$n_{2\text{-}5}$**, roots of nodose ganglia 2-5; **st**, supratemporal lateral line ganglion; **tr**, trigeminal ganglion; **va**, vestibuloacoustic ganglion; **v.ret.**, ventral retina.

Europe PMC Funders Author Manuscripts

Table 1

Degenerate primer sequences used to isolate fragments of *S. canicula* cDNAs.

Gene	Forward primer	Reverse primer	Annealing temp. °C
NeuroD	AAACGACGAGGACCTAAGAAGAARAARATGAC	TCGAACTCAGCAGATGGCTCRTGYTTRAA	61
Pax3	AGGAGACAGGCTCCATCAGA	GGGACAGAGCGTAATCAGTCTGNGGYTGRTG	55
Pax2	CACGGNGGNGTGAACCAGC	TYCCRGGNACCATKCCNGC	55
Phox2b	CAGGCTTCCGGATTCCARTAYAAYCC	GGAGGACAGCACGGAAGCRAANGGNCC	50
Eya4	ATGGAAATGCAGGATCTA	TAATACTGNGCRTACTG	55
Tbx3	CATCAGCCGCCRTTTTTCCC	CCATCGCCAACTTACTGGGG	55

Europe PMC Funders Author Manuscripts

Table 2

Putative placodal marker genes cloned for expression analysis in *S. canicula*.

Gene	Expected expression	Size (bp)	Equivalent amino acids of mouse homologue	Predicted amino acid identity to mouse homologue	GenBank Accession Number
NeuroD	Pan-neuronal	626	83-293	91% overall 98% in bHLH domain	EF185882
Pax3	Ophthalmic trigeminal placodes	944	92-415	82% overall 84% over partial Pax domain 98% in homeodomain	EF185883
Pax2	Otic and epibranchial placodes	898	24-344	78% overall 99% over partial Pax domain	EF185884
Phox2b	Epibranchial placode-derived neurons	691	38-297	75% overall 97% in homeodomain	EF185885
Eya4	Isolated in attempt to isolate *Eya1* as a pan-placodal marker	647	30-256	72% overall (59% to mouse Eya1)	EF185886
Tbx	Lateral line placodes	1435	35-506	65% overall 96% in T-box	EF185887

Notes: See Supplementary Figs 1-6 for protein alignments. References: *NeuroD*: Chae et al. (2004). *Pax3*: Stark et al. (1997). *Pax2*: Baker and Bronner-Fraser (2000); Ohyama and Groves (2004); Schlosser and Ahrens (2004). *Phox2b*: reviewed in Brunet and Pattyn (2002). *Eya1/4*: reviewed in Bailey and Streit (2006); Schlosser (2006). *Tbx3*: reviewed in Schlosser and Ahrens (2004).